



**TURUN  
YLIOPISTO**  
UNIVERSITY  
OF TURKU

# TOWARDS CYCLOPALLADATED THERAPEUTIC OLIGONUCLEOTIDES

---

Madhuri Ashok Hande





**TURUN  
YLIOPISTO**  
UNIVERSITY  
OF TURKU

# **TOWARDS CYCLOPALLADATED THERAPEUTIC OLIGONUCLEOTIDES**

---

Madhuri Ashok Hande

## **University of Turku**

---

Faculty of Science  
Department of Chemistry  
Chemistry  
Doctoral programme in Physical and Chemical Sciences

## **Supervised by**

---

Associate Professor Dr Tuomas Lönnberg  
Department of Chemistry  
University of Turku  
Turku, Finland

## **Reviewed by**

---

Professor Dr Eva Freisinger  
Department of Chemistry  
University of Zurich  
Switzerland

Professor Dr Leśnikowski Zbigniew Jan  
Laboratory of Medicinal Chemistry  
Institute of Medical Biology PAS  
Poland.

## **Opponent**

---

Professor Dr Anna Grandas  
Department of Inorganic and Organic Chemistry  
University of Barcelona  
Spain

The originality of this publication has been checked in accordance with the University of Turku quality assurance system using the Turnitin OriginalityCheck service.

ISBN 978-951-29-8672-9 (PRINT)  
ISBN 978-951-29-8673-6 (PDF)  
ISSN 0082-7002 (Print)  
ISSN 2343-3175 (Online)  
Painosalama, Turku, Finland 2021

*Dedicated To My Wonderful Family* ❤️

UNIVERSITY OF TURKU

Faculty of Science

Department of Chemistry

Chemistry

MADHURI HANDE: Towards Cyclopalladated Therapeutic Oligonucleotides

Doctoral Dissertation, 120 pp.

Doctoral Programme in Physical and Chemical Science

September 2021

## ABSTRACT

Based on Watson—Crick base pairing principle, therapeutic oligonucleotides bear the potential to either inhibit or alter protein synthesis. Replacing or augmenting Watson—Crick base pairing by metal coordination offers a promising way to increase the hybridization affinity of therapeutic oligonucleotides for target nucleic acids. Crosslinking of DNA by the anticancer agent cisplatin is a well-known example of utilization of metal—nucleic acid interactions for therapeutic purposes. Many other transition metal mediated interactions have also been widely studied but in most cases rapid ligand exchange makes applicability in the intracellular medium questionable. This thesis brings covalently palladated oligonucleotides in the light for the first time as a new addition to existing antisense techniques.

This thesis describes the synthesis of a few artificial nucleosidic and non-nucleosidic structures that offer reactive sites for cyclopalladation. The respective palladacyclic derivatives were integrated into short oligonucleotides and their base pairing preferences and effect on duplex stability studied by various techniques, including UV melting experiments (with detailed thermodynamic analysis), CD spectroscopy and Förster resonance energy transfer (FRET) –based competition assay. Pd(II) mediated base pairing in duplexes was found to depend on the structure of organometallic residue, the base pairing partner and the location of the base pair within the oligonucleotide. The palladated oligonucleotides were also tested for their splice correction ability in three human cell lines. In HeLa cells, the palladacyclic oligonucleotide modestly outperformed the corresponding unmodified oligonucleotide.

**KEYWORDS:** palladium, organometallic, palladacycle, oligonucleotide, base pairing, coordination, splice correction

TURUN YLIOPISTO

Matemaattis-luonnontieteellinen tiedekunta

Kemian laitos

Kemia

Madhuri Hande: Towards Cyclopalladated Therapeutic Oligonucleotides

Väitöskirja, 120 s.

Fysikaalisten ja kemiallisten tieteiden tohtoriohjelma

Syyskuu 2021

## TIIVISTELMÄ

Watson—Crick –emäspariutumiseen perustuvat oligonukleotidilääkkeet kykenevät estämään tai muuttamaan proteiinisynteesiä. Watson—Crick –emäspariutumisen korvaaminen tai täydentäminen on lupaava keino lisätä oligonukleotidilääkkeiden affiniteettia kohdenukleiinihappoihin. Syöpälääke sisplatiinin aiheuttama DNA:n ristiinsilloittuminen on hyvin tunnettu esimerkki metallien ja nukleiinihappojen välisten vuorovaikutusten hyödyntämisestä lääketieteessä. Monia muitakin siirtymämetallien välittämiä vuorovaikutuksia on tutkittu mutta useimmissa tapauksissa soveltuvuus solunsisäiseen käyttöön on kyseenalaista nopean ligandinvaihdon vuoksi. Tämä väitöskirjatyö on ensimmäinen tutkimus mahdollisuudesta käyttää kovalenttisesti palladoituja oligonukleotideja antisense-sovelluksissa.

Väitöskirjassa kuvataan joidenkin sellaisten nukleosidisten ja ei-nukleosidisten rakenteiden synteesi, joissa on syklopalladaatioon sopiva reaktiivinen paikka. Vastaavat palladasykliset johdokset liitettiin osaksi lyhyitä oligonukleotideja ja niiden emäspariutumistaipumuksia sekä vaikutusta kaksoiskiirteen pysyvyyteen tutkittiin CD- ja UV-sulamismittauksin (sisältäen yksityiskohtaisen termodynaamisen analyysin) sekä käyttäen Försterin resonanssienergiansiirtoon (FRET) perustuvaa kilpailukoetta. Pd(II)-välitteisen emäspariutumisen kaksoiskierteessä havaittiin riippuvan palladasyklin rakenteesta, vastinemäksestä sekä emäsparin sijainnista. Myös palladoitujen oligonukleotidien kykyä korjata virheellinen silmukoituminen testattiin kolmessa ihmisen solulinjassa. HeLa-solulinjassa palladasyklinen oligonukleotidi toimi vähän paremmin kuin vastaava modifioimaton oligonukleotidi.

ASIASANAT: palladium, organometallinen, palladasykli, oligonukleotidi, emäspariutuminen, koordinaatio, silmukoinnin korjaus

# Table of Contents

<b>Abbreviations .....</b>	<b>8</b>
<b>List of Original Publications .....</b>	<b>10</b>
<b>List of Related Publications .....</b>	<b>11</b>
<b>1 Introduction.....</b>	<b>12</b>
1.1 Biological significance of nucleic acids .....	12
1.1.1 Basic principle of Watson—Crick base pairing .....	12
1.1.2 Hoogsteen Base Pairing.....	14
1.1.3 Interactions of Metals with Nucleic Acids.....	15
1.2 Oligonucleotide Therapeutics .....	17
1.2.1 Antisense oligonucleotides .....	18
1.2.2 MicroRNAs.....	18
1.2.3 Splice switching Oligonucleotides (SSOs).....	19
1.2.4 Antigene Oligonucleotides.....	19
1.2.5 Aptamers.....	19
1.2.6 RNA Vaccines.....	20
1.3 Structural Modification of therapeutic oligonucleotides .....	22
1.3.1 Sugar Modifications.....	22
1.3.2 Backbone Modifications .....	23
1.3.3 Base Modifications .....	24
1.4 Nucleic Acid Metallation .....	25
<b>2 Aims of Thesis .....</b>	<b>28</b>
<b>3 Results and Discussions .....</b>	<b>29</b>
3.1 Synthesis of Phosphoramidite Building Blocks and Metallated Oligonucleotides .....	29
3.1.1 Synthesis of the Benzylamine Building Block .....	29
3.1.2 Synthesis of the cyclopalladated benzylamine .....	30
3.1.3 Synthesis of the protected aminooxymethyl C-nucleoside .....	31
3.1.4 Synthesis of cyclopalladated and mercurated oligonucleotides .....	31
3.2 UV melting studies of cyclopalladated, mercurated and unmetallated oligonucleotides .....	36
3.3 CD Melting studies of cyclopalladated, mercurated and unmetallated oligonucleotides .....	48
3.4 Thermodynamic Analysis of Melting Curves.....	49



3.5	Fluorescence Studies of cyclopalladated and unpalladated oligonucleotides .....	51
3.6	Splice-Correction.....	53
3.6.1	Lipofectamine 2000 Mediated Transfection .....	54
3.6.2	Gymnosis .....	55
3.7	Cytotoxicity Assay .....	56
<b>4</b>	<b>Conclusion .....</b>	<b>57</b>
<b>5</b>	<b>Experimental .....</b>	<b>59</b>
5.1	General Methods.....	59
5.2	Oligonucleotide Synthesis .....	59
5.3	UV Melting and CD Melting Temperature Studies .....	60
5.4	Fluorescence Studies.....	60
5.5	Biological Experiments .....	61
5.5.1	Cell Lines and Culture Conditions .....	61
5.5.2	Transfection by Lipofectamine 2000 .....	61
5.5.3	Gymnosis .....	61
5.5.4	Luciferase Assay .....	61
5.5.5	RNA Expression Analysis.....	62
5.5.6	Cell Viability Assay .....	62
5.5.7	Data Analysis .....	62
	<b>Acknowledgements .....</b>	<b>63</b>
	<b>List of References.....</b>	<b>66</b>
	<b>Original Publications.....</b>	<b>71</b>

# Abbreviations

2'-F	2'-Fluoro
2'-MOE	2'- <i>O</i> -methoxyethyl
2'-OMe	2'- <i>O</i> -methyl
A	adenosine
AMO	antagomir oligonucleotide
ASO	Antisense oligonucleotide
C	cytidine
CD	circular dichroism
CPG	controlled pore glass
dA	2'-deoxyadenosine
dC	2'-deoxycytidine
DCA	dichloroacetic acid
DCM	dichloromethane
dG	2'-deoxyguanosine
DMSO	dimethyl sulfoxide
DMTr	4,4'-dimethoxytrityl (4,4'-dimethoxytriphenylmethyl)
DNA	Deoxyribonucleic Acid
ds	double-stranded
dT	2'-deoxythymidine
dU	2'-deoxyuridine
ESI-MS	Electrospray Ionization Mass Spectrometry
FRET	Förster Resonance Energy Transfer
G	guanosine
GNA	Glycol Nucleic Acid
HG	Hoogsteen
HMBC	Heteronuclear Multiple Bond Correlation
HPLC	High Performance Liquid Chromatography
HRMS	High Resolution Mass Spectrometry
HSQC	Heteronuclear Single Quantum Coherence
LNA	Locked Nucleic Acid (a bridge between 2' oxygen and 4' carbon locks the ribose ring in the 3'- <i>endo</i> conformation)

miRNA	micro Ribonucleic Acid
mRNA	messenger Ribonucleic Acid
NMR	Nuclear Magnetic Resonance
ON	oligonucleotide
PS	phosphorothioate
Py	pyridine
RNA	Ribonucleic Acid
RP HPLC	Reverse Phase High Performance Liquid Chromatography
rt	room temperature
SELEX	Systematic Evolution of Ligands by EXponential enrichment
siRNA	Small interfering RNA
SSO	Splice Switching Oligonucleotide
T	Thymidine
TBDMS	<i>tert</i> -butyldimethylsilyl
tcDNA	tricycle DNA
TEA	triethylamine
TEAA	triethylammonium acetate
TFO	triplex forming oligonucleotide
THF	tetrahydrofuran
$T_m$	Melting Temperature
Tr	trityl (triphenylmethyl)
U	uridine
UNA	Unlocked Nucleic Acid (a ribose analogue lacking the bond between C2' and C3')
UV	ultraviolet
WC	Watson—Crick

# List of Original Publications

This dissertation is based on the following original publications, which are referred to in the text by their Roman numerals:

- I Hande M., Maity S., and Lönnberg T.: Palladacyclic Conjugate Group Promotes Hybridization of Short Oligonucleotides. *International Journal of Molecular Sciences*, 2018; 19: 1588.
- II Hande M., Saher O., Lundin K. E. Lundin, Smith C. I. E., Zain R., and Lönnberg T. Oligonucleotide–Palladacycle Conjugates as Splice-Correcting Agents. *Molecules*, 2019; 24: 1180.
- III Maity S., Hande M., and Lönnberg T.: Metal-Mediated Base Pairing of Rigid and Flexible Benzaldoxime Metallacycles. *ChemBioChem*, 2020; 21: 2321.
- IV Hande M., Maity S., and Lönnberg T.: Sequence dependence of Pd(II)-mediated base pairing by palladacyclic nucleobase surrogates. *Journal of Inorganic Biochemistry*, 2021; 222: 111506.

The original publications have been reproduced with the permission of the copyright holders.

# List of Related Publications

- I. Ukale D., Maity S., Hande M., and Lönnberg T.: Synthesis and Hybridization Properties of Covalently Mercurated and Palladated Oligonucleotides. *Synlett*, 2019; 30(15): 1733.
- II. Lönnberg T., Hande M., and Ukale D.: Oligonucleotide Complexes in Bioorganometallic Chemistry. *Reference Module in Chemistry, Molecular Sciences and Chemical Engineering*, 2021: DOI [10.1016/B978-0-12-820206-7.00030-5](https://doi.org/10.1016/B978-0-12-820206-7.00030-5)

# 1 Introduction

## 1.1 Biological significance of nucleic acids

Nucleic acids, deoxyribonucleic acid (DNA) and ribonucleic acid (RNA) are naturally occurring polymers, which are essential for life. They play vital roles in cell division and protein synthesis. DNA is responsible for storage and transfer of genetic information whereas RNA translates it to make proteins. Messenger RNA (mRNA) carries genetic information from DNA, transfer RNA (tRNA) brings amino acids to ribosomes and ribosomal RNA (rRNA) is responsible for translation of this information in protein formation.<sup>1,2</sup> Other types of RNA, known collectively as noncoding RNA (ribozymes, small nuclear RNA, microRNA (miRNA), small interfering RNA (siRNA)), have a significant contribution in molecular biology, including catalysis and gene regulation.<sup>3,4</sup>

### 1.1.1 Basic principle of Watson—Crick base pairing

Watson and Crick elucidated the structure of double helical DNA.<sup>5</sup> A nucleotide is the smallest functional unit of DNA and therefore each nucleotide is associated with genetic information. Each nucleotide comprises a phosphate group, a sugar and a nitrogenous heterocyclic base. DNA and RNA both contain a five-carbon sugar, 2'-deoxyribose in the former and ribose in the latter. A phosphodiester linkage connects the 3'- and 5'-carbons of two sugar units and its anionic nature offers nucleic acids high water solubility. The bases come in four varieties and act as the functional element of nucleic acids, carrying the genetic information. Three of the bases, adenine (A), cytosine (C) and guanine (G) are common to both DNA and RNA, whereas the fourth one is thymine (T) in DNA and uracil (U) in RNA (**Figure 1**).

Nucleobases have the ability to bind with their complementary partner. When two nucleic acid strands are mixed, single-stranded DNA or RNA binds antiparallel to its complementary strand by hydrogen bonds in a process termed as nucleic acid hybridization. In Watson—Crick base pairing between the complementary bases, adenine pairs with thymine by two hydrogen bonds and guanine pairs with cytosine by three hydrogen bonds. Each hydrogen bond involves a donor from one nucleobase

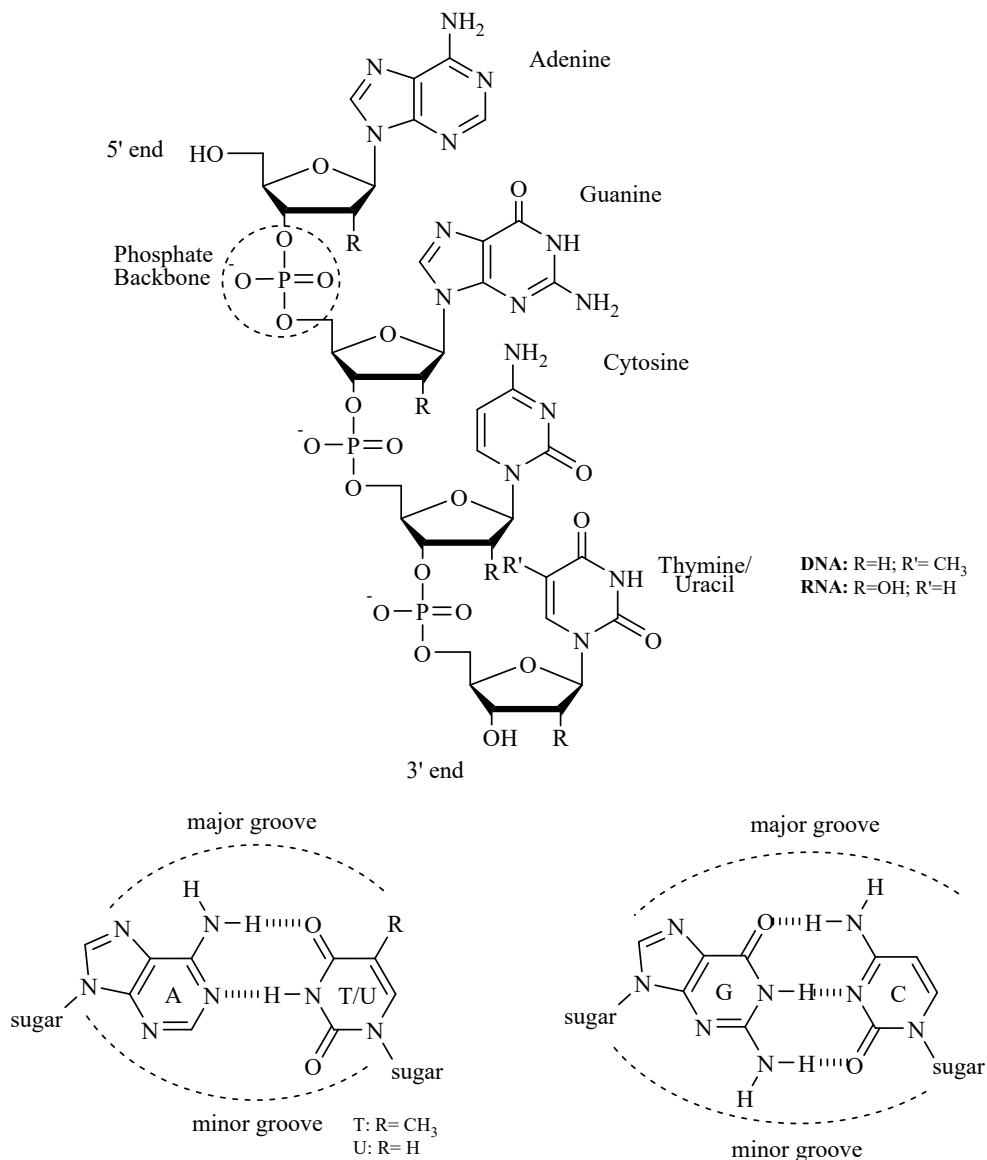


**Figure 1.** Structure of Nucleic Acid, DNA: R=H and R'=CH<sub>3</sub>; RNA: R= OH and R'= H. (B) Watson—Crick base pairing between G•C and A•T (hydrogen bonding denoted by dotted lines)

and an acceptor from another nucleobase. NH and NH<sub>2</sub> functions act as hydrogen bond donors whereas carbonyl oxygen and deprotonated endocyclic nitrogen act as hydrogen bond acceptors (**Figure 1**). Moreover, Watson—Crick base pairs are characterized by size complementarity, the large purine bases binds to the small pyrimidine bases. Watson—Crick base pairing forms the basis of recognition of complementary nucleic acid sequences. Mixing two complementary nucleic acid

strands leads to either a DNA•DNA, a DNA•RNA or a RNA•RNA double helix, depending on the sequences.

Major molecular biological processes such as replication, transcription and translation rely on Watson—Crick base pairing. Predictable hybridization based on simple rules of Watson—Crick base pairing also makes the design of a therapeutic oligonucleotide complementary to a given target sequence a straightforward task.

When a double-helical nucleic acid is heated, hydrogen bonding is disrupted and the constituent strands dissociate. Cooling of the same solution leads to reformation of the double helical structure. The former process is called denaturation and the latter renaturation. The temperature at which half of the duplexes are denatured is defined as the melting temperature ( $T_m$ ). Base pairing preferences play an important role in the stability of a double helix and especially with short duplexes even a single mispair results in a measurable drop in the melting temperature. Several important applications in the field of drug discovery, ranging from diagnosis to therapy, would benefit from increased hybridization affinity.<sup>6</sup>

### 1.1.2 Hoogsteen Base Pairing

Higher order nucleic acid structures, e.g. triple helix, quadruplex etc., exhibit various alternative modes of hydrogen bonding. Double stranded DNA formed by Watson—Crick base pairing can bind to a third strand of nucleic acid by Hoogsteen base pairing (**Figure 2**). The third strand binds to the major groove of dsDNA, resulting in a triple helical structure. A purine-rich central strand is crucial for the formation of triple helices as only purines have two surfaces for hydrogen bonding. Hoogsteen base pairing creates alternative DNA conformations that play role in recognition and replication.<sup>7</sup> Double stranded DNA is also an attractive target in therapeutics, in which case a third strand could be used e.g. to induce damage.

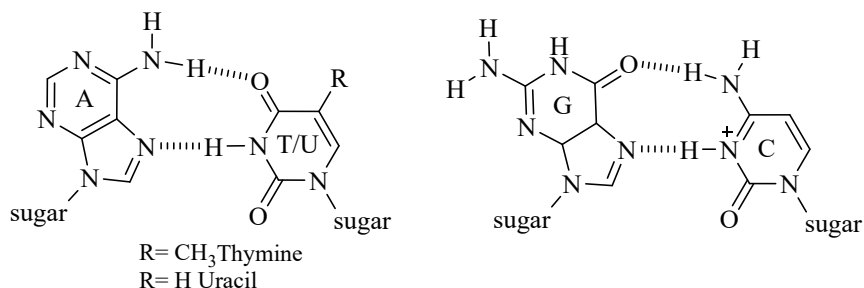


**Figure 2.** Hoogsteen base pairing between **A•T** and **G•C** (hydrogen bonding denoted by dotted lines)



### 1.1.3 Interactions of Metals with Nucleic Acids

Metals play a dynamic role in biological processes owing to their redox activity, various coordination modes and reactivity towards organic molecules. They assist in interactions between proteins and nucleic acids. Quite often, water molecules mediate interactions between nucleic acids and metals. For the sake of charge compensation, polyamines (spermines and spermidine) and metal ions (mono- or divalent) are essential to maintain the helical conformation of nucleic acids. Interaction between metal species and nucleic acids can be broadly divided into two classes, non-covalent interactions and coordinative interactions.<sup>8,9</sup> The former includes electrostatic attraction, intercalation, hydrogen bonding,  $\pi$ - $\pi$  interactions and weak van der Waals forces. The latter, in turn, include interactions between a metal ion and any ligand having active donor sites. Various factors, including the nature and charge of the metal ion, length and type of the nucleic acid, polarity of the solvent, the type of buffer (when applicable) and ionic strength of the solution, control metal—ligand interactions.<sup>10</sup> Hard metal ions binds to hard donors, e.g. oxygen, and soft metal ions binds to soft donors, e.g. sulphur and nitrogen. The scope of interactions between metal complexes and nucleic acids was evaluated deeply after 1965 when this mechanism found significant in cancer treatment.<sup>11</sup>

At physiological pH, the negatively charged phosphate backbone is neutralized by mainly alkali and alkaline earth metals. Elements of the 3d transition series (Sc(II), Ti(II), V(II), Cr(II), Fe(II), Co(II), Ni(II), Cu(II), Zn(II)) also interact with phosphate backbone in the order of decreasing softness. The ribose/deoxyribose sugar moiety of nucleic acids is the poorest ligand for coordination<sup>12</sup> though binding has been observed with Ca(II), Sr(II), Ba(II), Cu(II) and Mn(II) as well as some heavy metal ions, such as La(III), Ce(III), Pr(III), Sm(III), Gd(III) and Tb(III). Unprotonated endocyclic N atoms and exocyclic carbonyl O atoms of the natural purine and pyrimidine nucleobases, on the other hand, are obvious metal binding sites. Metal coordination sites of adenine and guanine are N1, N3, N7 and N1, N3, N7 and O7, respectively, whereas cytosine interacts with metal ions through N3, N4 and O2. Thymine and uracil both bind to metal ions via N3, O2 and O4. For the formation of metal-carbon bonds, C5 position of the pyrimidine bases (C and U) and C8 position of the purine bases is preferred (**Figure 3**).

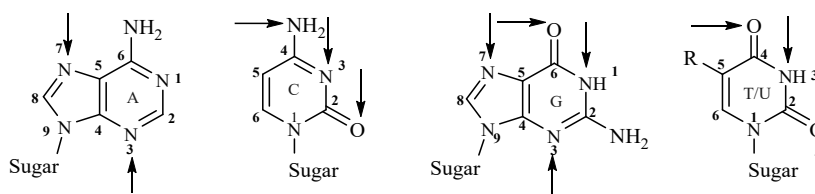


**Figure 3.** Potential metal binding sites of natural nucleobases indicated by arrows.

When hydrogen bonds between complementary nucleobases are formally replaced by coordinate bonds to a common metal ion, the interaction is termed as metal-mediated base pairing. Canonical, non-canonical, matched and mismatched base pairs all offer sites for metal ion coordination. Metal mediated base pairing is one of the most efficient ways for site-specific functionalization of nucleic acids. It has been studied widely with DNA and less extensively with RNA,<sup>13–15</sup> Glycol Nucleic Acid<sup>13,16</sup> (GNA) and Peptide Nucleic Acid<sup>13,17,18</sup> (PNA). Notably, metal-mediated site-specific interactions between nucleobases can efficiently generate intrastrand or interstrand crosslinks.<sup>19</sup> Such metal–ligand interactions influence the structure, conformation, stability and electronic properties of nucleic acids.<sup>10</sup> Katz reported the first metal-mediated base pair T-Hg(II)-T, between two natural thymine nucleobases (**Figure 4a**).<sup>20</sup> One metal–ligand coordination bond replaces two or three hydrogen bonds, which thus affects the stability of the duplex.<sup>21</sup> With the natural nucleobases, canonical Watson–Crick base pairing can compete with metal-mediated base pairing and hence compromise selectivity. In principle, coordinative bonds are stronger than non-covalent bonds although a strong nucleophile can displace a metal ion engaged in a coordination complex.<sup>8</sup>

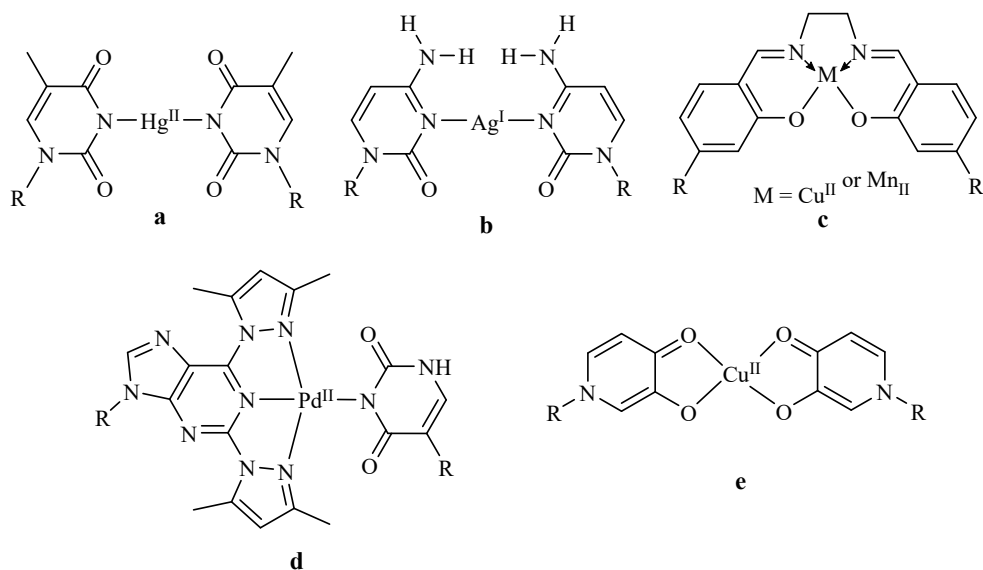


**Figure 4.** Illustrative examples of metal mediated base pair.

Often, metals preferring linear coordination geometry (such as Ag (I) and Hg (II)) have been chosen for bridging of two bases from different strands of nucleic acids but square planar coordination (such as with Mn(II), Cu(II), Ni(II), Pd(II) and Pt(II)) is also feasible.<sup>22</sup> T-Hg(II)-T and C-Ag(I)-C (**Figure 4a** and **b**) are the two most

extensively studied metal mediated base pair. Integration of Mn(II) and Cu(II) mediated base pair (**Figure 4c**) formed by a versatile ligand *N,N'*-bis(salicylidene)ethylenediamine brought significant stability to DNA duplexes.<sup>23</sup> Another artificial nucleoside, 2,6-bis(3,5-dimethylpyrazol-1-yl)purine ribonucleoside not only forms Pd(II) mediated base pair (**Figure 4d**) selectively with thymidine but also promoted duplex stability.<sup>24</sup> Interestingly, Shinoya et. al. reported a Cu(II) mediated five consecutive base pairs (**Figure 4e**) formed by artificial nucleobases.<sup>25</sup> The metal ion may displace a proton from the donor atom and different nucleobases have different preferences for coordination of metal ions. For instance, Ag(I) preferentially binds to GC rich sequences and Hg(II) to AT rich sequences. Likewise, interaction of cisplatin with DNA involves strong binding of Pt(II) to guanine and this interaction is likely responsible for mode of action.<sup>26</sup>

Potential metalation sites on natural nucleobases are not limited to the electronegative atoms. Organometallic nucleobases involving a M-C bond, where C is part of the nucleobase, are also feasible. Organometallic modification confers nucleobases novel properties beneficial for site-specific functionalization. The M-C bond in organometallic complexes can, in principle, be synthetically achieved by three methods, including i) ligand-directed C-H activation, ii) C-H cleavage and iii) C-X oxidative addition.<sup>27</sup>

## 1.2 Oligonucleotide Therapeutics

Oligonucleotides (relatively short stretches of nucleic acids) bear potential to treat a wide range of diseases by various mechanisms. The idea of controlling gene expression was first introduced by Stephenson and Zamecnik in 1978.<sup>28</sup> The majority of oligonucleotide drugs recognize their target by Watson—Crick base pairing. They can target either DNA, RNA or proteins to treat diseases arising from genetic, viral or bacterial origin, including malignant tumours.<sup>29</sup> Apart from complementary base pairing, they can interact with proteins by folding into elaborate tertiary structures.

Oligonucleotide therapeutics can be highly specific to target disease relevant DNA (antigene oligonucleotides), RNA (ASOs, miRNAs and SSOs) or non-nucleic acid targets such as proteins (aptamers).<sup>30</sup> Different targets require different chemical constructions. Drugs to target RNA have been further classified based on action of mechanism as antisense oligonucleotides (ASOs), micro RNAs, single interfering RNAs and DNazymes. Till date, fourteen oligonucleotide drugs have been approved by FDA.<sup>31</sup>

### 1.2.1 Antisense oligonucleotides

Antisense oligonucleotides<sup>32,33,34</sup> are single-stranded oligonucleotides which are complimentary to a messenger RNA. They are potentially useful in therapeutics for their gene silencing ability. Instead of targeting proteins to modulate their functionality by conventional drugs, ASO drugs bind to the corresponding mRNA target and inhibit translation of genes into proteins.<sup>35</sup> **(Figure 5)** ASOs act by either steric blocking or enzymatic catalysis<sup>36</sup> (translational inhibition or enzymatic cleavage) where RNase H selectively cleaves the RNA strand in RNA-DNA hetroduplexes. ASOs have great potential in treatment of inflammatory diseases, viral diseases and cancer because differences in genetic profile exist between healthy and diseased individuals.<sup>37</sup> ASOs are the oldest approach for using oligonucleotides as therapeutic agents. The first FDA approved antisense drug Vitravene was developed by Ionis Pharmaceuticals in August 1998.

### 1.2.2 MicroRNAs

RNA interference (RNAi) is a cellular process that uses the sequence of a gene itself to turn it off. Usually double stranded RNA triggers RNAi. MicroRNAs (miRNAs) are class of non-coding RNA usually containing 19-25 bases that regulate gene expression post-transcriptionally by hybridizing with the 3'-untranslated regions of mRNA. Like ASOs, miRNAs bind to a complementary mRNA sequence, affecting either post-translational repression or degradation and silencing **(Figure 5)**. miRNAs have a key role in cellular differentiation, apoptosis, immune response and proliferation. Their dysregulation results in diseases such as inflammatory and viral diseases, as well as cancer.<sup>38,39</sup> Some miRNAs may act as oncogenes whereas others are tumour-suppressing. miRNA drugs are based on two different strategies: i) antimRNAs or antagomirs (AMOs) and ii) miRNA mimics (miR-mimics).

AMOs are endogenous, small non-coding RNAs that are generally a perfect match to a miRNA target. These single-stranded molecules sterically block the mature miRNA from binding to its mRNA target.<sup>40</sup> In some cases, AMOs are used to target precursor miRNA to inhibit miRNA maturation.<sup>41</sup> Chemically modified AMOs are efficient in gene silencing of dysregulated miRNA owing to their improved binding affinity and biostability. One significant advantage of using miRNA (over siRNA) is that one single miRNA can regulate multiple gene targets from the same family.<sup>42</sup> miR-mimics are non-natural RNA-like double stranded molecules designed for gene silencing. miRNA mimics substitute a lost miRNA and restore the normal function, such as tumour suppression.<sup>43</sup>

### 1.2.3 Splice switching Oligonucleotides (SSOs)

Pre-mRNA splicing is the process of removing introns from pre-messenger RNA and ligating together exons to produce a mature messenger RNA (mRNA) that is further translated into proteins (**Figure 5**). Splicing can be inhibited by the hybridization of an oligonucleotide to the 5' and 3' regions involved in this process. SSOs are chemically modified short antisense oligonucleotides designed to bind pre-mRNA, inhibiting incorrect and/or restoring correct protein synthesis. Many severe diseases, such as sickle-cell anemia or muscular dystrophy, are caused by translation of a defective protein and splice switching appears the only feasible treatment.<sup>44,45</sup>

### 1.2.4 Antigene Oligonucleotides

Antigene strategy is an attractive gene silencing method for treating viral diseases and cancer. A triplex forming oligonucleotide (TFO) called antigene binds to double stranded DNA by Hoogsteen or reverse Hoogsteen hydrogen bonding. It has been demonstrated that TFOs are able to recognize polypurine/polypyrimidine stretches in the major groove of double stranded DNA, resulting in inhibition of transcription of the targeted gene (**Figure 5**). Besides restricting gene expression, antigene oligonucleotides also have the potential to modify gene function permanently.<sup>46,47</sup> Owing to the relative weakness of Hoogsteen and reverse Hoogsteen hydrogen bonding, modified TFOs with superior hybridization affinity are needed in antigene strategy.

### 1.2.5 Aptamers

Aptamers are short (20-100 nucleotides), chemically synthesized single-stranded DNA or RNA molecules that exhibit high affinity and selectivity for a given target (usually not a nucleic acid). They are often isolated *in vitro* by a process termed Systematic Evolution of Ligands by EXponential enrichment (SELEX). Aptamers bind to their targets by folding into a unique three-dimensional conformation that functionally resembles traditional antibodies (**Figure 5**). Aptamers have several attractive features compared to antibodies, such as smaller size, flexibility, high stability and internalization into cells. As their specificity and binding affinity depend on their three-dimensional structure, they do not necessarily interact through sequence-specific hybridization. They have several applications as drugs, diagnostic and a bioimaging agents, drug delivery agents and analytical reagents for food inspection and hazard detection.<sup>48</sup>

## 1.2.6 RNA Vaccines

RNA vaccines, an attractive new class of nucleic acid therapeutics, became one of the major success stories in the year 2020 after the coronavirus pandemic hit globally. Although mRNA vaccines had been studied before for various viral infections such as rabies<sup>49</sup>, Zika<sup>50</sup>, cytomegalovirus<sup>51</sup>, and influenza<sup>52</sup>, Covid-19 has made mRNA vaccines crucial for our lives. The idea of injecting plasmid DNA or mRNA to produce a foreign protein was first demonstrated by Wolff and co-workers<sup>53</sup> in 1990. A short and specific fragment of viral RNA (mRNA) is first prepared by enzymatic polymerization. The mRNA is then delivered in lipid nanoparticles to prevent enzymatic degradation. Within the cell, the viral mRNA is used as instructions to prepare an antigen (a viral protein) and subsequently degraded (**Figure 5**). Presently, two mRNA based vaccine candidates have been approved for use in emergency in several countries including USA and Europe to prevent severe Covid-19 infection. They are developed by leading manufacturers Pfizer-BioNTech (Comirnaty) and Moderna (mRNA-1273).

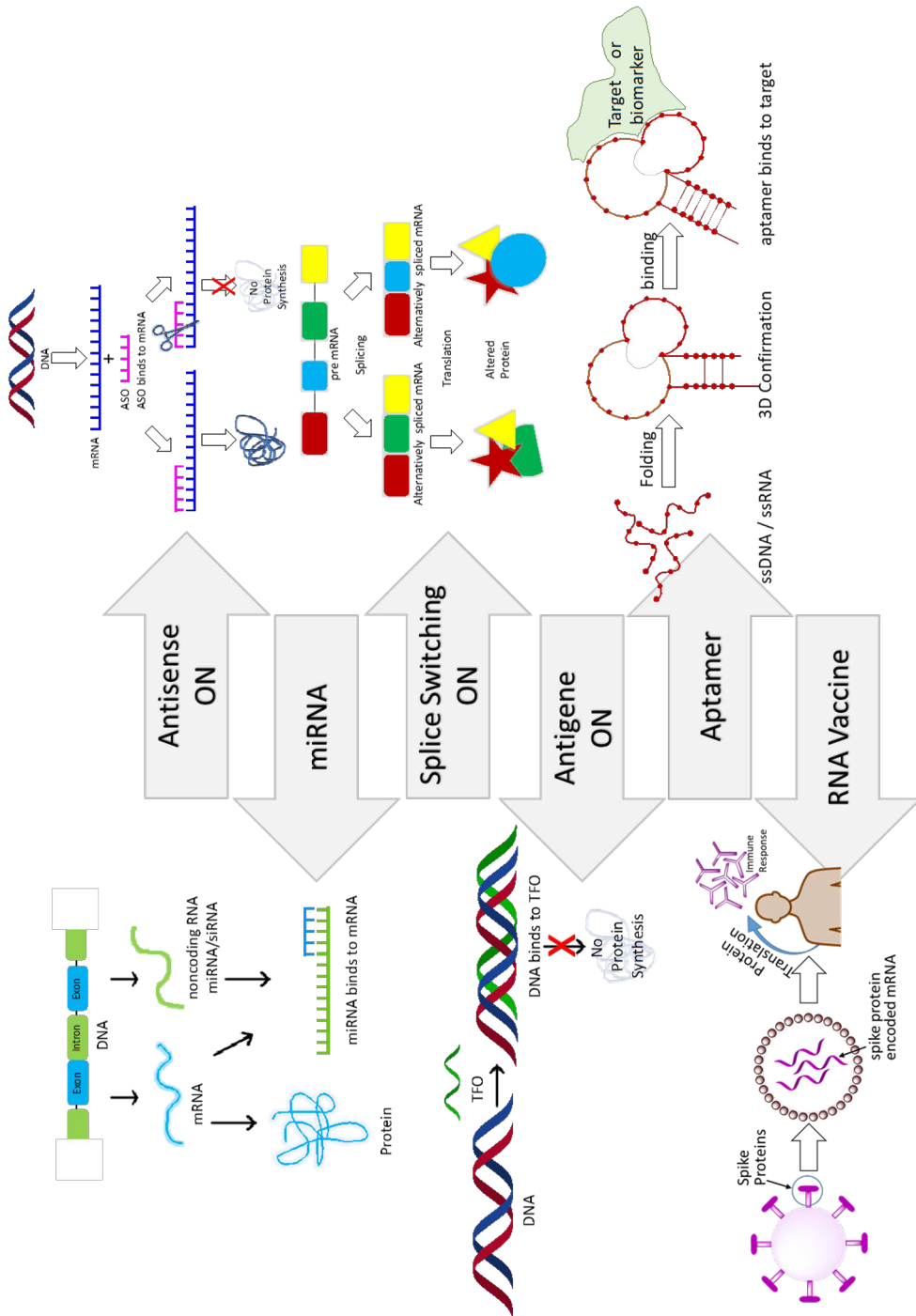


**Figure 5.** Schematic representation of various classes of oligonucleotide therapeutics. antisense oligonucleotides, microRNA, splice switching oligonucleotides, antigenic oligonucleotides, aptamers, and RNA vaccines.

## 1.3 Structural Modification of therapeutic oligonucleotides

A main drawback preventing extensive use of ON therapeutics is difficulty in successful delivery to target organs and tissues other than the liver.<sup>54</sup> Natural nucleic acids are extremely vulnerable to nuclease degradation. Their pharmacokinetic profile is poor and they exhibit weak affinity to plasma proteins. A therapeutic oligonucleotide should also have a high hybridization affinity to a complementary nucleic acid sequence. Most of the RNA from cells forms more stable RNA•RNA than RNA•DNA duplexes, making unmodified DNA oligonucleotides unsuitable for therapeutic purposes. All of these issues can be addressed by appropriately modified synthetic oligonucleotides.<sup>55</sup> Thus, chemical modification is an important approach to regulate the functions of many biomolecules.<sup>36</sup>

Various chemical modifications to enhance hybridization affinity to the target site, increase resistance to nucleases and promote cellular uptake have been developed till date. This research has mainly focused on 2'-modifications of the ribose sugar, artificial nucleic acids bearing more extensively modified sugar analogues, phosphodiester replacement, and base modifications.

### 1.3.1 Sugar Modifications

Chemical modifications at the 2'-position of the ribose sugar have the ability to modulate the structural, functional and biological properties of RNA oligonucleotides. Such modifications can improve duplex stability, nuclease resistance and immune stimulation. Several modifications such as 2'-fluoro (2'-F), 2'-*O*-methyl (2'-OMe), 2'-*O*-methoxyethyl (2'-OME), Locked Nucleic Acids (LNA: a ribose analogue where 2'-O and 4'-C atoms are linked by a methylene bridge), tricyclo DNA (tcDNA) and Unlocked Nucleic Acids (UNA: a ribose analogue lacking the bond between the C2' and C3' atoms) (**Figure 6**) have been widely studied in order to demonstrate their efficacy<sup>56,57,58</sup>. These modifications were designed for different purposes. For example, LNA and tcDNA modifications reduce conformational flexibility of the nucleotides and thus increase the binding affinity through preorganization into the favourable *C*<sub>3</sub>-*endo* conformation.<sup>59</sup> The *C*<sub>3</sub>-*endo* conformation can also be promoted by introducing 2'-OMe or 2'-MOE modifications. 2'-F modification enhances hybridization affinity as well as provides resistance against metabolic degradation when used with phosphorothioate (PS) backbone.



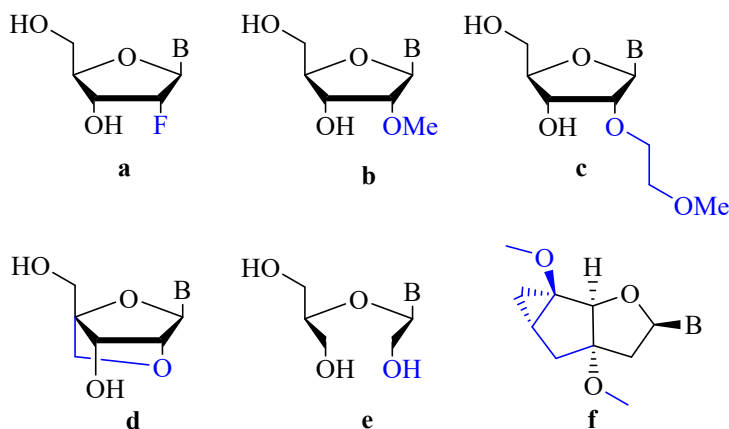


**Figure 6.** Representation of 2'-modified pentose sugars in RNA: a) 2'-F; b) 2'-OMe; c) 2'-OME; d) LNA; e) UNA; f) tcDNA.

### 1.3.2 Backbone Modifications

Extensive efforts have been directed to modify the native internucleotide linkage to obtain resistance to enzymatic cleavage while at the same time retaining the ability to activate RNase H. Many alternative linkages, including phosphorothioate, boranophosphate, methylphosphonate, amide, methylene, formacetal, thioformacetal and sulfonyl (**Figure 7**) have been studied.<sup>60–63</sup>

Substitution of one of the non-bridging oxygen atoms of a natural phosphodiester linkage with sulphur gives rise to a phosphorothioate linkage. Phosphorothioate remains one of the most successful backbone modifications despite its greater binding to proteins and nonspecific effects in cells and side effects *in vivo*. Moreover, phosphorothioate backbone significantly reduces the hybridization affinity to target mRNA.<sup>29,64</sup>

Gryaznov and coworkers<sup>65</sup> developed the N3'→P5' phosphoramidate modification in which 3'-oxygen of the 2'-deoxyribose ring was substituted by an amino group. Oligonucleotides with these modifications have proven to form stable duplexes and triplexes with complementary ssRNAs and dsDNAs featuring a polypurine tract, respectively. The 3'-amino group also makes them resistant to nucleases in addition to contributing positively to duplex stability. However, despite its potent antisense activity in cell culture this linkage fails to activate RNase H when bound to its complementary target.<sup>61,62,65</sup>

Methylphosphonate linkage was introduced as an uncharged linkage where methyl group replaces a non-bridging oxygen. Although methylphosphonate modified ASOs are highly resistant to nucleases, their poor aqueous solubility,

inability to activate RNase H and poor affinity to complementary targets made them less attractive to explore as therapeutic agents.

Morpholino oligonucleotides are an example of a more extensive modification, a morpholine ring replacing the sugar and a phosphorodiamidate group replacing the native phosphodiester bond. Morpholino oligonucleotides are comparatively cost effective as well as easy to assemble. They have proven more efficient than phosphorothioate-modified oligonucleotides in cell free assays as well as in some cultured cells.<sup>62,66</sup> These results suggest that they are sequence specific and do not bind non-specifically to proteins. They act by steric blocking and do not activate RNase H.

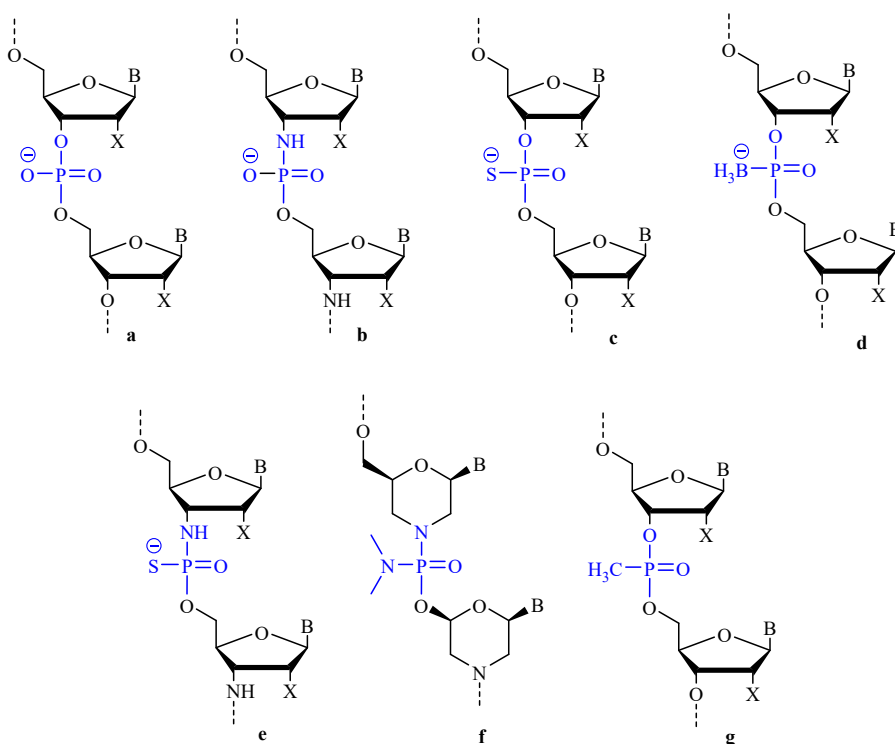


**Figure 7.** Natural and modified internucleosidic linkages: a) natural phosphodiester linkage; b) N3'→P5' phosphoramidate linkage; c) phosphorothioate linkage; d) boranophosphate linkage; f) morpholino DNA; g) methylphosphonate linkage. x can be H, OH or any substituent mentioned in the **Figure 6**.

### 1.3.3 Base Modifications

To widen the range of applications of DNA scaffolds, base moieties have been modified to carry fluorophores, ligands for metal ions, helix stabilizers and shape mimics of DNA bases.<sup>67</sup> In the beginning, modified pyrimidine and purine bases

were designed with the expectation that they would improve the duplex stability by additional hydrogen bonds, electrostatic interactions, hydrophobicity or  $\pi$ - $\pi$  stacking interactions.<sup>68</sup> Fully artificial constructs have also been introduced to replace the base moiety. Modifications can be introduced either as modified phosphoramidite building blocks or post-synthetically on appropriately modified oligonucleotides.<sup>69,70</sup> If stability of the C-N glycosidic linkage is a concern, it can be replaced by a C-C linkage, giving rise to a C-nucleoside analogue.<sup>68</sup> Besides alternative hydrogen bonding patterns, base modifications can expand base pairing beyond conventional hydrogen-bonded base pairs.<sup>9</sup> For example, two bases on opposite strands can coordinate to a common metal ion in an interaction commonly referred to as metal-mediated base pairing.<sup>9</sup>

## 1.4 Nucleic Acid Metallation

Many transition metal complexes are important therapeutic agents, especially for the treatment of various types of cancer. The great success story started with the discovery of cisplatin, a simple square planar Pt(II) complex first synthesized<sup>71</sup> by M. Peyrone in 1844, followed by its chemical structure elucidation<sup>72</sup> by Alfred Werner in 1893. Rosenberg *et al.* in 1965 discovered inhibition of cell division in *Escherichia coli* by cisplatin, suggesting its potential as an antitumor agent.<sup>73</sup> Coordinative bond formation between Pt(II) and the most nucleophilic position of nuclear DNA (guanine N7) gives rise to a platinum cross-linked adduct that efficiently distorts the DNA structure and inhibits transcription.<sup>74</sup> In 1978, FDA approved cisplatin as an anticancer drug and to date most cancer treatments are based on cisplatin. Cisplatin acts by a DNA damaging mechanism which is inherently non-specific and thus also kills healthy cells. Therefore, despite being a great success story in the treatment of e.g. testicular cancer, cisplatin is not a universal treatment for all other types of cancer.<sup>74</sup>

Covalent interactions between opposite strands can greatly stabilize duplexes (or triplexes). Metal coordination is one of many ways to form such covalent interactions, and the possibility of using cisplatin-type crosslinks to promote hybridization of therapeutic oligonucleotides was studied extensively in the early 2000s.<sup>74</sup> For example, 5-methylcytidine analogues with either thioether or imidazole modification placed next to each other within a 2'-O-Me ribonucleotide formed intrastrand crosslinks when treated with transplatin (a clinically inactive isomer of cisplatin)<sup>75</sup>. These intrastrand crosslinks arose through formation of Pt-S and Pt-N bonds. The intrastrand adduct, in turn, stimulated the sequence-specific formation of interstrand cross-links through rearrangement upon hybridization with complementary RNA and modulated gene expressions efficiently.<sup>76-78</sup> In another example, transplatin integrated into a Hoogsteen homopyrimidine strand stabilized

the triplex formed between this strand and a complementary Watson—Crick duplex, thus ruling out the possibility of displacement of the TFO by replication or transcription machinery.<sup>79</sup>

Solid phase DNA synthesis is hardly compatible with the direct incorporation of metallated building blocks. Peptide Nucleic Acid (PNA) synthesis, however, allows such assembly. Sequence-selective cross-linking was observed between transplatin-modified PNA and a complementary oligonucleotide, demonstrating potential as an antisense oligonucleotide.<sup>80</sup>

The kinetic inertness of Pt(II) means that the Pt(II) coordination products tend to be kinetic (rather than thermodynamic), making off-target binding a challenge. Coordinative complexes of labile metal ions, on the other hand, quickly dissociate under the highly diluted and metal-deficient conditions of the intracellular medium. Integrating organometallic nucleobases into oligonucleotides offers a way to combine rapid ligand exchange with high stability in physiological medium<sup>76-23</sup> although in practice the selection is limited by hydrolytic stability. The most extensively studied organometallic nucleic acids are those incorporating 5-mercuricytidine or -uridine residues. The mercurated pyrimidine nucleobases were prepared by electrophilic aromatic substitution at C-5 position.<sup>81</sup> At nucleotide and dinucleotide level, C-metallation has also been studied with Pt(II), Pt(III), Pd(II), Au(III), Rh(III) or Ir(III).<sup>82</sup>

Ligand-directed cyclometalation is a popular way of making carbon—metal bonds under mild conditions. The first organometallic nucleosides prepared through *N*-directed cyclometalation featured a 6-phenylpurine Ir(II) or Rh(III) metallacycle as the base moiety.<sup>83</sup> Respective dinucleotide derivatives were also synthesized successfully. Iridacycles have even been incorporated into oligonucleotides but only as a non-nucleosidic conjugate group tethered to the 5'-end through a flexible linker. A cyclometallated Ir(III) polypyridyl complex at the 5'-terminus of an oligonucleotide demonstrated improved ability to selectively hybridize with single- and double-stranded targets compared to the unconjugated oligonucleotide.<sup>84</sup> The Ir(III) oligonucleotide conjugate formed a stable duplex with single stranded 14-, 20- and 26-mer DNA oligonucleotides and a stable triplex with a double-stranded 14-mer DNA oligonucleotide. With longer (20- and 26-mer) dsDNA targets, no triplex stabilization was observed. Another Ir(III) complex,  $[\text{Ir}(\text{ppy})_2(\text{dppz})]^+$ , conjugated with DNA demonstrated higher melting temperature consistent with the conjugation.<sup>85</sup> Alike Ir(II), Ir(III) and Rh(III), cyclometallation of nucleosides were also explored by formation of Os(IV) metallacycles which have potential for further functionalization of oligonucleotides.<sup>86,87</sup>

Structural and thermodynamic similarities between Pt(II) and Pd(II) complexes as well as comparatively lower toxicity of Pd(II) complexes have stimulated the exploration of Pd(II) complexes as an alternative to Pt(II) complexes as anticancer

agents.<sup>88</sup> However, their ligand exchange is five orders of magnitude faster, resulting in rapid hydrolysis under physiological conditions. Cyclopalladated compounds have been studied to circumvent this problem in the case of small-molecule drugs and, given their easy synthetic accessibility, appear a feasible approach also in the case of oligonucleotides. The first artificial metal-mediated base pair was actually reported between two phenylenediamine *C*-nucleosides and Pd(II) already in 1999<sup>89</sup> but two decades later, Pd(II)-mediated base pairing within oligonucleotides still remains an underexplored field.

## 2 Aims of Thesis

Antisense technology was born in 1978 from the desire to achieve a therapeutic effect by intervening with the process of gene expression. Two decades later, FDA approved the first oligonucleotide-based drug, followed by thirteen others as of 2021. Over the years, oligonucleotide therapeutics has been extensively studied to diagnose and treat many life threatening diseases. Various approaches acting at different levels in the process of protein translation have emerged, such as RNA interfering, RNase mediated cleavage, splice-switching, non-coding RNA inhibition, gene activation and editing. Most oligonucleotide drugs identify their targets by hydrogen-bonded Watson—Crick base pairing.

Besides hydrogen bonding, nucleic acids can also be targeted by metal coordination, as exemplified by cisplatin and related anticancer agents. Such coordination can also be harnessed to enhance the stability of a nucleic acid duplex, such as the one between a therapeutic oligonucleotide and its target. Using kinetically labile metal ions instead of Pt(II) could decrease off-target binding but coordination complexes of such metal ions rapidly dissociate in the metal deficient intracellular medium. This problem can, in principle, be addressed by replacing coordination complexes with organometallic complexes. A great number of small molecule organometallic compounds have been studied for their potential as therapeutic agents but corresponding studies on organometallic oligonucleotides are scanty.

The aims of this thesis are:

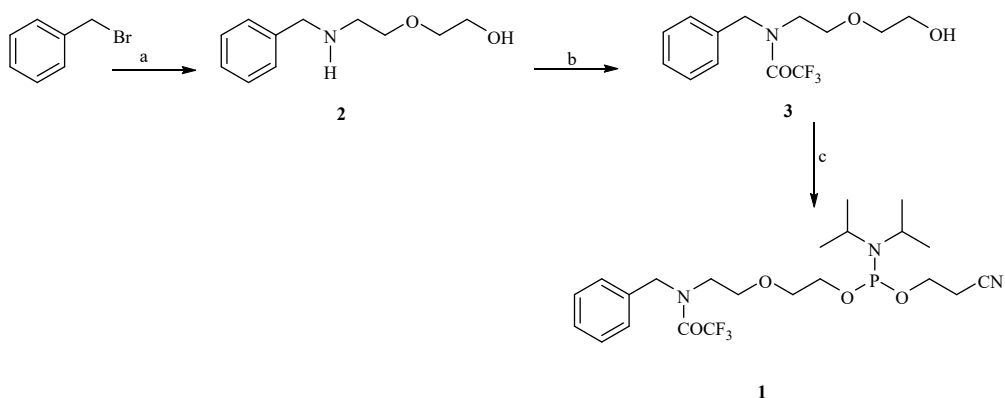
1. To develop a robust synthetic strategy for cyclopalladated oligonucleotides.
2. To gain insights into Pd(II) mediated base pairing within double-helical oligonucleotides.
3. To assess the applicability of cyclopalladated oligonucleotides as splice correcting agents.

## 3 Results and Discussions

### 3.1 Synthesis of Phosphoramidite Building Blocks and Metallated Oligonucleotides

#### 3.1.1 Synthesis of the Benzylamine Building Block

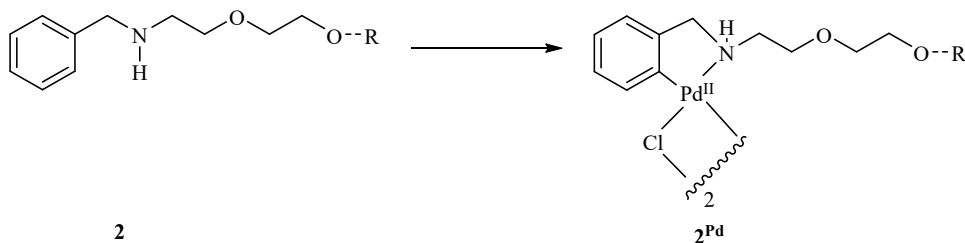
Synthesis of the protected benzylamine phosphoramidite building block **1** was achieved by the route outlined in **Scheme 1**. Benzyl bromide was treated with excess of 2-(2-aminoethoxy)ethanol to yield the secondary amine **2** which, in turn, was treated with ethyl trifluoroacetate to afford the trifluoroacetamide **3**. Intermediate **3** was phosphitylated by further treatment with 2-cyanoethyl-*N,N*-diisopropylchlorophosphoramidite to afford **1**. Phosphoramidite **1** was used for oligonucleotide synthesis without further purification.



**Scheme 1.** Synthesis of benzylamine phosphoramidite. Reagents and conditions: a) 2-(2-aminoethoxy)ethanol, MeCN, 25 °C, 16 h; b) ethyl trifluoroacetate, Et<sub>3</sub>N, MeOH, 25 °C, 16 h; c) 2-cyanoethyl-*N,N*-diisopropylchlorophosphoramidite, Et<sub>3</sub>N, CH<sub>2</sub>Cl<sub>2</sub>, N<sub>2</sub> atmosphere, 25 °C, 3 h.

### 3.1.2 Synthesis of the cyclopalladated benzylamine

Prior to cyclopalladation of modified oligonucleotides, optimal reaction conditions were established on the model compound 2-[2-(benzylamino)ethoxy]ethanol (**2**). Accordingly, compound **2** was treated with lithium tetrachloropalladate at room temperature in a 1:1 mixture of water and acetonitrile for 16 h to afford **2<sup>Pd</sup>**. Formation of **2<sup>Pd</sup>** was confirmed by NMR experiments that showed a loss of one *ortho* proton in <sup>1</sup>H NMR and downfield shift of the carbon directly attached to Pd(II) in <sup>13</sup>C NMR. In addition, the peaks corresponding to the remaining aromatic protons were split owing to loss of symmetry (2:2:1 for unmetallated benzylamine), consistent with the presence of the desired compound. <sup>1</sup>H, <sup>13</sup>C NMR and HRMS data were all consistent with the chloride-bridged dimer as shown in **Scheme 2**.



**Scheme 2.** Synthesis of cyclopalladated benzylamine **2<sup>Pd</sup>** and corresponding modified oligonucleotides **ON1b-Pd**, **ON2b-Pd**, **ON3b-Pd** and **ON4b-Pd**. Reagents and conditions: a) Li<sub>2</sub>PdCl<sub>4</sub>, MeCN, H<sub>2</sub>O, 25 °C, 16 h. (R Substituents are summarized in **Table 1**)

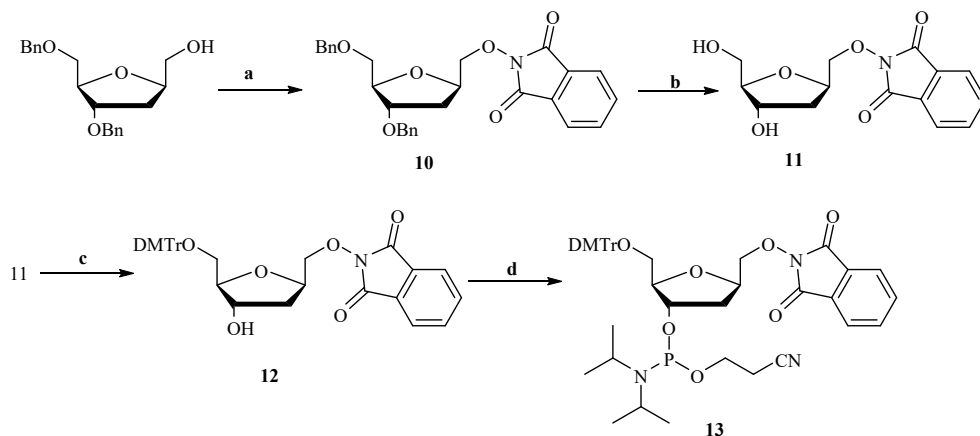
**Table 1.** R group in **Scheme 2** represents following substituents.

<b>2</b>	R=H	<b>2<sup>Pd</sup></b>	R=H
<b>ON1b</b>	R=5'-GCT CTG GC-3'	<b>ON1b-Pd</b>	R=5'-GCT CTG GC-3'
<b>ON2b</b>	R=5'-GCT CTG G-3'	<b>ON2b-Pd</b>	R=5'-GCT CTG G-3'
<b>ON3b</b>	R=5'-GCT CTG -3'	<b>ON3b-Pd</b>	R=5'-GCT CTG -3'
<b>ON4b</b>	R=5'-GCT CT-3'	<b>ON4b-Pd</b>	R=5'-GCT CT-3'
<b>ON6b</b>	R=5'- mC*mC*mU* mC*mU*mU* iA*mC*mC* mU*mC*mA* mG*mU*mU* mA*mC*mA*-3'	<b>ON6b-Pd</b>	R=5'- mC*mC*mU* mC*mU*mU* iA*mC*mC* mU*mC*mA* mG*mU*mU* mA*mC*mA*-3'
<b>ON7b</b>	R=5'- mC*mA*mG*mA*mG* iU*mU*mC*mU*mC*mA*mG* mG* mA*mU* mG*mU*mA*-3'	<b>ON7b-Pd</b>	R=5'- mC*mA*mG*mA*mG* iU*mU*mC*mU*mC*mA*mG* mG* mA*mU* mG*mU*mA*-3'

\*Represents internucleotide phosphorothioate linkages and **m** represents 2'-O-Me substituents on ribose sugar.



### 3.1.3 Synthesis of the protected aminooxymethyl C-nucleoside



**Scheme 3.** Synthesis of protected aminooxymethyl C-nucleoside and its phosphoramidite building block. Reagents and conditions: a) DIAD, HONPhth,  $\text{Ph}_3\text{P}$ , THF, 25 °C, 12 h; b)  $\text{Pd}(\text{OH})_2/\text{C}$ , EtOAc,  $\text{H}_2$  atmosphere, 25 °C, 1 h; c) DMTrCl, pyridine, 25 °C, 12 h; d) 2-cyanoethyl-*N,N*-diisopropylchlorophosphoramidite,  $\text{Et}_3\text{N}$ ,  $\text{CH}_2\text{Cl}_2$ ,  $\text{N}_2$  atmosphere, 25 °C, 2 h.

The phthaloyl-protected aminooxymethyl C-nucleoside phosphoramidite **13** was obtained as shown in **Scheme 3**. Mitsunobu reaction between 3, 5-di-*O*-benzyl-*C*-hydroxymethyl-2-deoxy- $\beta$ -*D*-ribofuranose and *N*-hydroxyphthalimide yielded the fully protected aminooxymethyl C-nucleoside **10**. Both benzyl protections were removed by  $\text{Pd}(\text{OH})_2/\text{C}$ -catalysed hydrogenation to yield **11**. Finally, 5'-dimethoxytritylation of C-nucleoside **11** followed by 3'-phosphitylation afforded the phosphoramidite building block **13**.

### 3.1.4 Synthesis of cyclopalladated and mercurated oligonucleotides

After the optimization of cyclopalladation of compound **2**, the same reaction was performed on oligonucleotides **ON1b**, **ON2b**, **ON3b**, **ON4b**, **ON6b** and **ON7b** to achieve cyclopalladated oligonucleotides **ON1b-Pd**, **ON2b-Pd**, **ON3b-Pd**, **ON4b-Pd**, **ON6b-Pd** and **ON7b-Pd**, respectively. All oligonucleotides were mixed in 1:1 mixture of water and acetonitrile with two equivalents of lithium tetrachloropalladate. All cyclopalladated oligonucleotides were purified by RP-HPLC and characterized by electrospray ionization mass spectrometry (ESI-MS), followed by quantification by UV spectrophotometer.

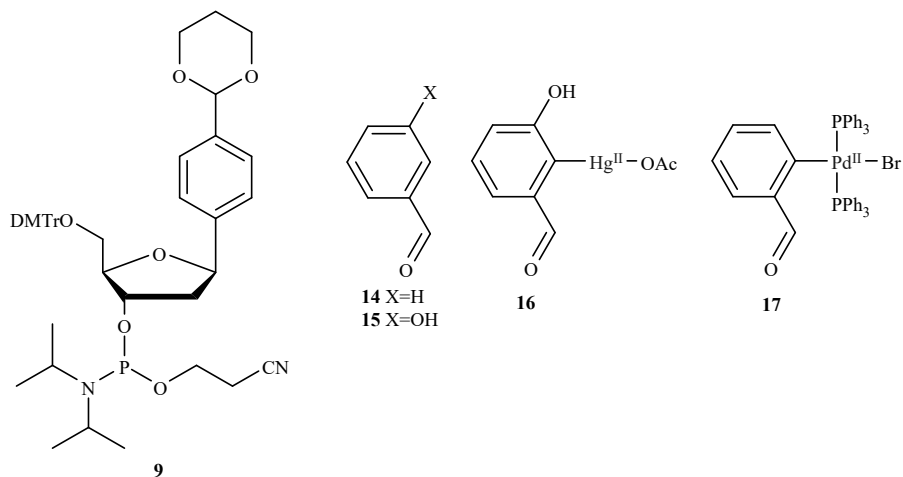
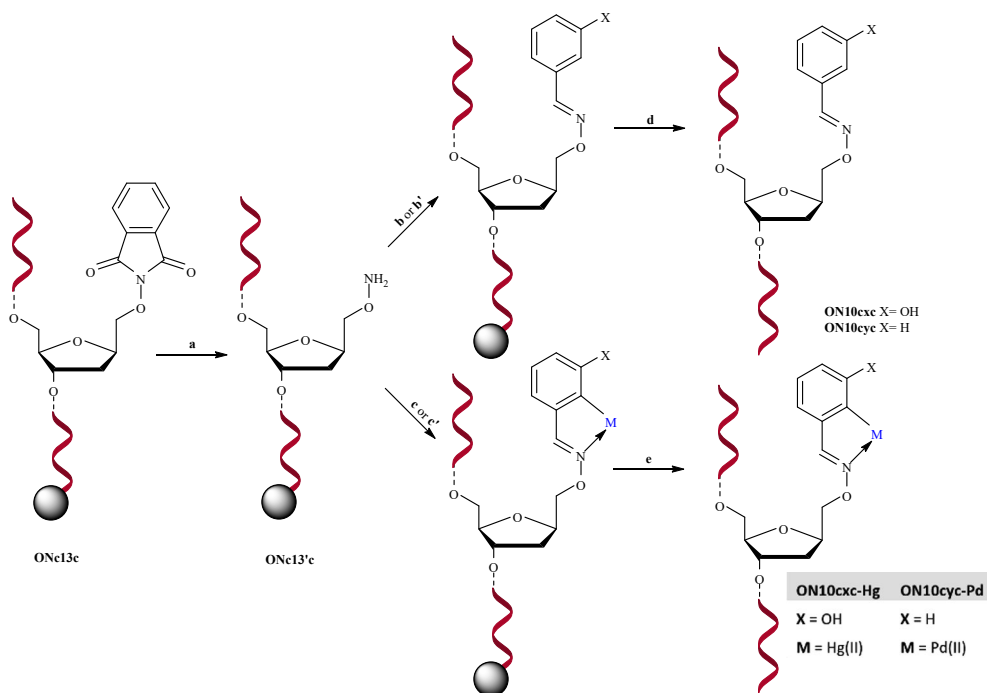


**Figure 8.** Structure of phosphoramidite **9**; benzaldehyde analogues **14**, **15**, mercurated benzaldehyde analogue **16**, and palladated benzaldehyde analogue **17**.

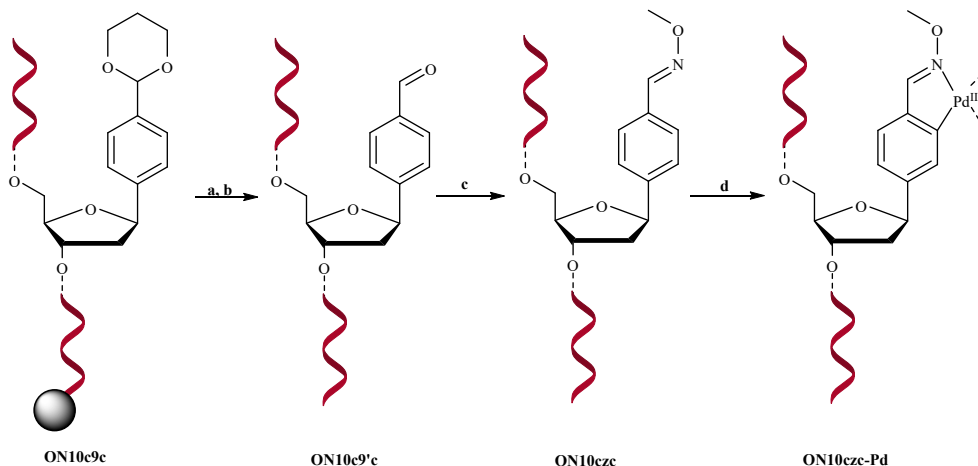
Synthesis of phosphoramidite **9** has been reported previously.<sup>90</sup> Protected benzaldehyde C-nucleoside phosphoramidite **9** and protected aminooxymethyl C-nucleoside phosphoramidite **13** were incorporated into oligonucleotides by an automated DNA/RNA synthesizer using conventional phosphoramidite strategy. 1,3-dioxolane and phthaloyl protections of oligonucleotides **ON10c9c** and **ON10c13c** were removed on support by treatment with dichloroacetic acid in  $\text{CH}_2\text{Cl}_2$  and hydrazine acetate in pyridine, respectively (**Scheme 4**). The exposed aminoxy functionality was immediately reacted with 3-hydroxybenzaldehyde (**14**) or benzaldehyde (**15**) to afford the desired oligonucleotides. Finally, conventional ammonolysis was performed on all oligonucleotides (**ON10cxc**, **ON10cyc** and **ON10c9c'**) to release them from solid support and to remove the base and phosphate protecting groups. Synthesis of the metallated oligonucleotides **ON10cxc-Hg** and **ON10cyc-Pd** has been reported previously in the same way by using either mercurated or palladated benzaldehydes.<sup>91</sup>



**Scheme 4.** Outline of synthesis of **ON10cxc**, **ON10cyc**, **ON10cxc-Hg** and **ON10cyc-Pd**. Reagents and Conditions: a)  $\text{H}_2\text{NNH}_2$ , AcOH, pyridine, 25 °C, 45 min; b) neat 3-hydroxy benzaldehyde, DMSO, 25 °C, 12 h; b') neat benzaldehyde, 25 °C, 12 h; c) 16, DMSO, 25 °C, 12 h; c') 17,  $\text{CH}_2\text{Cl}_2$ , 25 °C, 12 h; d) 25% aqueous ammonia, 55 °C, 12 h e)  $\text{MeNH}_2$ ,  $\text{NH}_3$ ,  $\text{H}_2\text{O}$ , 65 °C, 10 min.

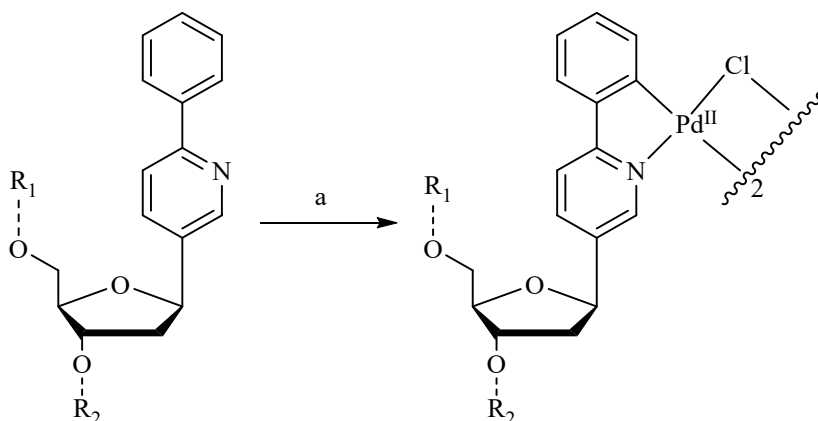
Post purification by RP-HPLC, **ON10czc** was obtained by treating **ON10c9c'** with an aqueous solution of methoxylamine. This treatment yielded a central *O*-methylbenzaldoxime (**ON10czc**) from benzaldehyde (**ON10c9c'**). Once **ON10czc** was purified by RP-HPLC, it was cyclopalladated by using lithium tetrachloropalladate in a mixture of water and acetonitrile to obtain **ON10czc-Pd**. Synthesis of **ON10czc-Pd** is outlined in **Scheme 5**.

Purification by RP-HPLC, characterization by ESI-MS and quantification by UV spectrophotometry of all oligonucleotides (**ON10c9c**, **ON10cxc**, **ON10cyc**, **ON10czc**, **ON10cxc-Hg**, **ON10cyc-Pd** and **ON10czc-Pd**) are thoroughly explained in the original publications.<sup>90,92,93</sup> Oximation of **ON10cxc** led to *E* and *Z* isomers that were separable by RP-HPLC and hence characterized separately.



**Scheme 5.** Preparation of cyclopalladated oligonucleotide **ON10czc-Pd**. Reagents and Conditions: a) 2% dichloroacetic acid,  $\text{CH}_2\text{Cl}_2$ ,  $25^\circ\text{C}$ , 2 h; b) 25% aq. ammonia,  $55^\circ\text{C}$ , 16 h; c) aqueous  $\text{CH}_3\text{ONH}_2\cdot\text{HCl}$ ,  $\text{NaOAc}$ ,  $\text{H}_2\text{O}$ ; d)  $\text{Li}_2\text{PdCl}_4$ ,  $\text{MeCN}$ ,  $\text{H}_2\text{O}$ ,  $25^\circ\text{C}$ , 16 h.

Synthesis of the 2-phenylpyridine *C* nucleoside, its phosphoramidite building block and corresponding unpalladated and cyclopalladated oligonucleotides have been reported previously<sup>94</sup> and the same procedures were followed to prepare **ON10pcc-Pd** and **ON10ccp-Pd** (Scheme 6). All oligonucleotides (**ON10pcc**, **ON10ccp**, **ON10pcc-Pd** and **ON10ccp-Pd**) were purified by RP-HPLC, characterized by ESI-MS and quantified by UV spectrophotometry.



**ON10pcc:**  $\text{R}_1 = \text{H}$ ;  $\text{R}_2 = 5\text{'-GA GCC CTG GC-3'}$

**ON10ccp:**  $\text{R}_1 = 5\text{'-CGA GCC CTG G-3'}$ ;  $\text{R}_2 = \text{H}$

**ON10cpc:**  $\text{R}_1 = \text{R}_2 = \text{H}$

**ON10pcc-Pd:**  $\text{R}_1 = \text{H}$ ;  $\text{R}_2 = 5\text{'-GA GCC CTG GC-3'}$

**ON10ccp-Pd:**  $\text{R}_1 = 5\text{'-CGA GCC CTG G-3'}$ ;  $\text{R}_2 = \text{H}$

**ON10cpc-Pd:**  $\text{R}_1 = \text{R}_2 = \text{H}$

**Scheme 6.** Palladation of 2-Phenylpyridine modified oligonucleotide. Reagents and Conditions: a)  $\text{Li}_2\text{PdCl}_4$ ,  $\text{NaOAc}$ ,  $\text{MeOH}$ ,  $\text{H}_2\text{O}$ ,  $55^\circ\text{C}$ .

**Table 2** represent the  $m/z$  values of modified oligonucleotides along with their retention times in RP HPLC. No demetallation was observed during chromatographic purification. Furthermore, UV melting profiles of the palladacyclic oligonucleotides between 10 and 90 °C were reproducible over at least three heating and cooling cycles, indicating stability of the modifications in aqueous solution.

**Table 2.** Mass and retention time data of modified oligonucleotides.

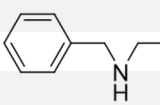
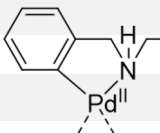
Oligonucleotides		Calculated $m/z$	Observed $m/z$	Retention Time (min)
<b>ON1b</b>	[M-2H] <sup>2-</sup>	1327.7573	1328.26	7.5 <sup>[a]</sup>
<b>ON2b</b>	[M-2H] <sup>2-</sup>	1183.2341	1183.2387	7 <sup>[a]</sup>
<b>ON3b</b>	[M-2H] <sup>2-</sup>	1018.7079	1019.2082	6 <sup>[a]</sup>
<b>ON4b</b>	[M-2H] <sup>2-</sup>	854.1816	854.1886	1.9 <sup>[a]</sup>
<b>ON1b-Pd</b>	[M-2H] <sup>2-</sup>	1380.2051	1379.6852	15 <sup>[a]</sup>
<b>ON2b-Pd</b>	[M-2H] <sup>2-</sup>	1235.682	1235.1907	15.1 <sup>[a]</sup>
<b>ON3b-Pd</b>	[M-2H] <sup>2-</sup>	1071.1557	1070.6747	15.1 <sup>[a]</sup>
<b>ON4b-Pd</b>	[M-2H] <sup>2-</sup>	906.6294	906.1424	15.1 <sup>[a]</sup>
<b>ON6b</b>	[M-3H] <sup>3-</sup>	2122.2265	2122.2223	14 <sup>[b]</sup>
<b>ON6b-Pd</b>	[M-4H] <sup>3-</sup>	2156.8558	2156.9644	16.5 <sup>[b]</sup>
<b>ON7b</b>	[M-3H] <sup>3-</sup>	2183.2438	2183.2366	14 <sup>[b]</sup>
<b>ON7b-Pd</b>	[M-4H] <sup>3-</sup>	2217.8731	2217.9622	17 <sup>[b]</sup>
<b>ON10pcc</b>	[M-2H] <sup>2-</sup>	1679.31	1679.8579	13.5 <sup>[c]</sup>
<b>ON10pcc-Pd</b>	[M-3H] <sup>3-</sup>	1154.1719	1154.5068	12.5 <sup>[c]</sup>
<b>ON10ccp</b>	[M-2H] <sup>2-</sup>	1639.31	1679.8447	13 <sup>[c]</sup>
<b>ON10ccp-Pd</b>	[M-3H] <sup>3-</sup>	1154.1719	1154.5012	13-13.5 <sup>[c]</sup>
<b>ON10cxc</b> Faster Eluting Isomer	[M-2H] <sup>2-</sup>	1677.3049	1677.7947	21 <sup>[d]</sup>
<b>ON10cxc</b> Slower Eluting Isomer	[M-2H] <sup>2-</sup>	1677.3049	1677.8156	21.5 <sup>[d]</sup>
<b>ON10cyc</b>	[M-2H] <sup>2-</sup>	1669.3075	1669.7942	21.5 <sup>[d]</sup>
<b>ON10czc</b>	[M-2H] <sup>2-</sup>	1669.3075	1669.8142	20.5 <sup>[d]</sup>
<b>ON10czc-Pd</b>	[M-2H] <sup>2-</sup>	1721.7553	1721.8109	19.5-283 <sup>[d]</sup>

RP-HPLC purification protocol: Hypersil ODS C18 column (250 × 4.6 mm, 5 μm) eluting with a linear gradient **[a]** 0 to 30% over 25 min of MeCN in 50 mM aqueous TEAA; **[b]** 0 to 50% over 30 min of MeCN in 50 mM aqueous TEAA; **[c]** 5 to 30% over 30 min of MeCN in 50 mM aqueous TEAA; **[d]** 5–30 % over 30 min of MeCN in 50 mM aqueous TEAA. Detailed protocols can be found in original publications.<sup>90,95–97</sup>

### 3.2 UV melting studies of cyclopalladated, mercurated and unmetallated oligonucleotides

Impact of organopalladated residues at variable positions (5'- or 3'-end or in the middle of the sequence) on the hybridization affinity of short oligonucleotides was evaluated by UV melting experiments. All oligonucleotide sequences used in these experiments are outlined in **Table 3**.

**Table 3.** Oligonucleotide sequences used in UV melting, CD melting, Fluorescence and *in vitro* studies.

Oligonucleotide	Sequences	
ON1a	5' - AGC TCT GGC-3'	 <p style="text-align: center;"><b>2</b></p>
ON2a	5' - AGC TCT GG-3'	
ON3a	5' - AGC TCT G-3'	
ON4a	5' - AGC TCT -3'	
ON1b	5' - 2GC TCT GGC-3'	 <p style="text-align: center;"><b>2<sup>Pd</sup></b></p>
ON2b	5' - 2GC TCT GG-3'	
ON3b	5' - 2GC TCT G-3'	
ON4b	5' - 2GC TCT -3'	
ON1b-Pd	5' - 2 <sup>Pd</sup> GC TCT GGC-3'	
ON2b-Pd	5' - 2 <sup>Pd</sup> GC TCT GG-3'	
ON3b-Pd	5' - 2 <sup>Pd</sup> GC TCT G-3'	
ON4b-Pd	5' - 2 <sup>Pd</sup> GC TCT -3'	
ON6	5'-mC*mC*mU* mC*mU*mU*mA*mC*mC*mU*mC*mA* mG*mU*mU*mA*mC*mA*-3'	
ON6b	5'-2*mC*mC*mU* mC*mU*mU*mA*mC*mC*mU*mC*mA* mG*mU*mU*mA*mC*mA*-3'	
ON6b-Pd	5'-2 <sup>Pd</sup> *mC*mC*mU* mC*mU*mU*mA*mC*mC*mU*mC*mA* mG*mU*mU*mA*mC*mA*-3'	
ON7	5' -mC*mA*mG* mA*mG*mU*mU*mC*mU* mC*mA*mG* mG*mA*mU* mG*mU*mA*-3'	
ON7b	5' - 2*mC*mA*mG* mA*mG*mU*mU*mC*mU* mC*mA*mG* mG*mA*mU* mG*mU*mA*-3'	
ON7b-Pd	5' - 2 <sup>Pd</sup> *mC*mA*mG* mA*mG*mU*mU*mC*mU* mC*mA*mG* mG*mA*mU* mG*mU*mA*-3'	
ON8	5'-rArUrU rGrUrA rArCrU rGrArG rGrUrA rArGrA rGrGrU rU-3'	
ON9	5'- ATT GTA ACT GAG GTA AGA GGT T-3'	
ON5gag	5'- GCC AGA GCT CG-3'	
ON5agg	5'- ACC AGG GCT CG-3'	
ON5cgg	5'- CCC AGG GCT CG-3'	
ON5gcg	5'- GCC AGC GCT CG-3'	
ON5gga	5'- GCC AGG GCT CA-3'	

Oligonucleotide	Sequences	
ON5ggc	5'- GCC AGG GCT CC-3'	
ON5ggg	5'- GCC AGG GCT CG-3'	
ON5ggt	5'- GCC AGG GCT CT-3'	
ON5gtg	5'- GCC AGT GCT CG-3'	
ON5tgg	5'- TCC AGG GCT CG-3'	
ON10c9c	5'- CGA GC <sup>9</sup> CTG GC-3'	
ON10cac	5'- CGA GCA CTG GC-3'	
ON10pcc	5'- PGA GCC CTG GC-3'	
ON10pcc-Pd	5'- P <sup>Pd</sup> GA GCC CTG GC-3'	
ON10cpc	5'- CGA GCP CTG GC-3'	
ON10cpc-Pd	5'- CGA GCP <sup>Pd</sup> CTG GC-3'	
ON10ccp	5'- CGA GCC CTG GP-3'	
ON10ccp-Pd	5'- CGA GCC CTG GP <sup>Pd</sup> -3'	
ON10cxc	5'- CGA GCX CTG GC-3'	
ON10cxc-Hg	5'- CGA GCX <sup>Hg</sup> CTG GC-3'	
ON10cyc	5'- CGA GCY CTG GC-3'	
ON10cyc-Pd	5'- CGA GCY <sup>Pd</sup> CTG GC-3'	
ON10czc	5'- CGA GCZ CTG GC-3'	
ON10czc-Pd	5'- CGA GCZ <sup>Pd</sup> CTG GC-3'	
ON5gag-Fam	5'- Fam-GCC AGA GCT CG-3'	
ON5gcg-Fam	5'- Fam-GCC AGC GCT CG-3'	
ON5ggg-Fam	5'- Fam-GCC AGG GCT CG-3'	
ON5gtg-Fam	5'- Fam-GCC AGT GCT CG-3'	
ON10cac-Dabcyl	5'- CGA GCA CTG GC-Dabcyl-3'	
ON10ccc-Dabcyl	5'- CGA GCC CTG GC-Dabcyl-3'	
ON10cgc-Dabcyl	5'- CGA GCG CTG GC-Dabcyl-3'	
ON10ctc-Dabcyl	5'- CGA GCT CTG GC-Dabcyl-3'	

\*Represents internucleotide phosphorothioate linkages, r represents ribose sugar and m represents 2'-O-Me substituents on ribose sugar.

The benzylamine moiety, tethered to the oligonucleotide through a flexible diethylene glycol spacer, offers a site for ligand-directed palladation. This non-nucleosidic modification was incorporated at the 5'-terminus. Hybridization affinity of **ON1b-Pd**, **ON2b-Pd**, **ON3b-Pd** and **ON4b-Pd** was tested by mixing each of them with each of the natural counterparts **ON5gag**, **ON5gcg**, **ON5ggg** and **ON5gtg**. Additionally, oligonucleotides containing an unmetallated benzylamine (**ON1b**, **ON2b**, **ON3b**, and **ON4b**) or adenine residue (**ON1a**, **ON2a**, **ON3a** and **ON4a**) at

the 5'-terminus were used to compare the hybridization affinity between metallated and unmetallated oligonucleotides to their target. **Figure 9** represents the summary of experiment. Pd(II) mediated base pairing in case of artificial nucleobases into short oligonucleotides, either 2'-O-methyl RNA<sup>24</sup> or GNA,<sup>98</sup> selectively pair with thymine by enhancing duplex stability than its unmetallated frameworks. Taking into account the preference of Pd(II) mediated base pairing to thymine, the 5'-residue (i.e. cyclopalladated benzylamine moiety, benzylamine moiety or adenine) in each case, was placed opposite to a thymine residue of a TCG trinucleotide overhang. Except for the central nucleobase, the unmodified parts of the duplexes were complementary to each other. Hence, placing a single mismatched nucleobase in the target sequence, a few nucleobases away from the 5'-modification represents a rational model to evaluate the fidelity of hybridization.

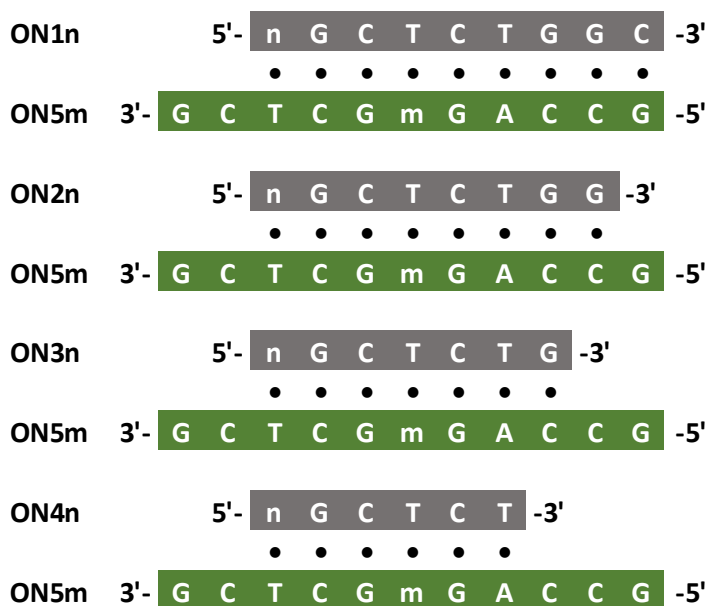


**Figure 9.** Schematic representation of UV Melting experiments by mixing **ON1n**, **ON2n**, **ON3n**, **ON4n** with **ON5m**. **ON1n** represents **ON1b**, **ON1b-Pd** and **ON1a**; **ON2n** represents **ON2b**, **ON2b-Pd** and **ON2a**; **ON3n** represents **ON3b**, **ON3b-Pd**, and **ON3a**; **ON4n** represents **ON4b**, **ON4b-Pd** and **ON4a**. **ON5m** represents **ON5gag**, **ON5gcg**, **ON5ggg** and **ON5gtg**. • represents Watson—Crick base pairing.

The longest matching duplexes, **ON1a•ON5gag**, **ON1b•ON5gag** and **ON1b-Pd•ON5gag**, exhibited sigmoidal UV melting curves (**Figure 11**), with melting temperatures of  $40.4 \pm 0.7$ ,  $35.8 \pm 0.6$  and  $41.0 \pm 0.1$  °C, respectively. **ON1b-Pd•ON5gag** was also modestly stabilized compared to **ON1a•ON5gag**, having an additional A•T Watson—Crick base pair at the 5'-terminus. The shorter duplexes,



in turn, did not fully hybridize at temperatures above 10 °C. Melting temperatures of all duplexes are summarized **Table 4** and **Figure 10**. Notably, irrespective of the length and sequence, no natural or modified oligonucleotide yielded a sigmoidal melting profile upon hybridization with **ON5gag**. With longer mismatched duplexes, melting temperatures could be determined even though complete hybridization was not achieved over the temperature range used. In addition, neither the cyclopalladated benzylamine oligonucleotides nor their unmetallated counterparts hybridized with the mismatched target sequences **ON5gag**, **ON5ggg** or **ON5gtg**.

**Table 4.** UV Melting temperature (°C) of duplexes formed by **ON1b**, **ON2b**, **ON3b**, **ON4b**, **ON1b-Pd**, **ON2b-Pd**, **ON3b-Pd**, **ON4b Pd**, **ON1a**, **ON2a**, **ON3a** and **ON4a** with **ON5gag**, **ON5gagc**, **ON5ggg** and **ON5gtg**; pH = 7.4 (20 mM cacodylate buffer); [oligonucleotides] = 3.0 μM; I(NaClO<sub>4</sub>) = 0.10 M. [2-Mercaptoethanol] (ME) = 100 μM.

	ON5gag	ON5gag + ME	ON5gagc	ON5gagc + ME	ON5ggg	ON5ggg + ME	ON5gtg	ON5gtg + ME
<b>ON1a</b>	40.4 ± 0.7	40.8 ± 0.6	n.a. <sup>1</sup>	n.a. <sup>1</sup>	17.6 ± 0.4	16.2 ± 0.7	17.9 ± 0.3	15.5 ± 0.3
<b>ON1b</b>	35.8 ± 0.6	34.9 ± 1.1	n.a. <sup>1</sup>	n.a. <sup>1</sup>	16.0 ± 0.7	16.8 ± 0.6	16.9 ± 0.4	15.5 ± 1.1
<b>ON1b-Pd</b>	41.0 ± 0.1	38.3 ± 0.9	n.a. <sup>1</sup>	n.a. <sup>1</sup>	22.6 ± 0.4	17.3 ± 0.8	22.4 ± 0.7	15.3 ± 0.7
<b>ON2a</b>	31.8 ± 1.3	30.9 ± 1.2	n.a. <sup>1</sup>	n.a. <sup>1</sup>	n.a. <sup>1</sup>	n.a. <sup>1</sup>	n.a. <sup>1</sup>	n.a. <sup>1</sup>
<b>ON2b</b>	30.5 ± 1.3	29.3 ± 0.8	n.a. <sup>1</sup>	n.a. <sup>1</sup>	n.a. <sup>1</sup>	n.a. <sup>1</sup>	n.a. <sup>1</sup>	n.a. <sup>1</sup>
<b>ON2b-Pd</b>	32.7 ± 1.0	30.2 ± 0.1	n.a. <sup>1</sup>	n.a. <sup>1</sup>	n.a. <sup>1</sup>	n.a. <sup>1</sup>	n.a. <sup>1</sup>	n.a. <sup>1</sup>
<b>ON3a</b>	21.0 ± 0.9	19.0 ± 0.5	n.a. <sup>1</sup>	n.a. <sup>1</sup>	n.a. <sup>1</sup>	n.a. <sup>1</sup>	n.a. <sup>1</sup>	n.a. <sup>1</sup>
<b>ON3b</b>	20.5 ± 0.8	20.0 ± 0.9	n.a. <sup>1</sup>	n.a. <sup>1</sup>	n.a. <sup>1</sup>	n.a. <sup>1</sup>	n.a. <sup>1</sup>	n.a. <sup>1</sup>
<b>ON3b-Pd</b>	21.2 ± 1.2	19.3 ± 0.3	n.a. <sup>1</sup>	n.a. <sup>1</sup>	n.a. <sup>1</sup>	n.a. <sup>1</sup>	n.a. <sup>1</sup>	n.a. <sup>1</sup>
<b>ON4a</b>	16.1 ± 0.4	17.3 ± 1.0	n.a. <sup>1</sup>	n.a. <sup>1</sup>	n.a. <sup>1</sup>	n.a. <sup>1</sup>	n.a. <sup>1</sup>	n.a. <sup>1</sup>
<b>ON4b</b>	15.4 ± 0.8	17.0 ± 0.8	n.a. <sup>1</sup>	n.a. <sup>1</sup>	n.a. <sup>1</sup>	n.a. <sup>1</sup>	n.a. <sup>1</sup>	n.a. <sup>1</sup>
<b>ON4b-Pd</b>	15.7 ± 0.8	17.6 ± 0.9	n.a. <sup>1</sup>	n.a. <sup>1</sup>	n.a. <sup>1</sup>	n.a. <sup>1</sup>	n.a. <sup>1</sup>	n.a. <sup>1</sup>

<sup>1</sup> No sigmoidal melting curve was obtained

2-Mercaptoethanol is a strong ligand for soft transition metal ions, including Pd(II). UV melting experiments were repeated in the presence of 100 μM 2-mercaptoethanol to gain more information on the origin of the observed stabilization by the palladacyclic benzylamine residue relative to its unpalladated counterpart. The presence of a competing ligand in the system is expected to disrupt coordination between Pd(II) and nucleobases which was the presumed reason behind the increased thermal stability. As expected, the melting temperature of duplex **ON1b-Pd•ON5gag** significantly dropped to 38.3 ± 0.9 °C. This drop indicates that cyclopalladated benzylamine interacted with the thymine containing trinucleotide overhang through Pd(II) coordination, thus enhancing hybridization affinity. Melting temperatures of duplexes formed by **ON1b-Pd** with **ON5ggg** and **ON5gtg** also

dropped upon addition of 2-mercaptoethanol, by 5 and 7 °C, respectively. Similar destabilization upon addition of a competing ligand was observed also in the case of the shorter matched duplexes formed by **ON5gag**. With all target sequences, the affinity drop was bigger with the palladacyclic oligonucleotides than their unmetallated counterparts. Besides disruption of Pd(II) coordination, 2-mercaptoethanol could decrease the  $T_m$  by making the cyclopalladated benzylamine moiety sterically more demanding and thus more difficult to adapt into the double helix.

To study their impact on hybridization of longer sequences more relevant for antisense or splice-switching applications, cyclopalladated benzylamine and its unmetallated counterpart were incorporated at the 5'-terminus of 19-mer 2'-*O*-methyl-RNA phosphorothioate oligonucleotides. These oligonucleotides (**ON6b** and **ON6b-Pd**) were designed to hybridize with the native RNA oligonucleotide **ON8**. Similar experiments were carried out on negative control oligonucleotides **ON7b** and **ON7b-Pd**, having no sequence complementarity with **ON8**. Unmodified oligonucleotides **ON6** and **ON7** were also used as positive and negative controls, respectively.

UV melting curves of duplexes **ON6•ON8**, **ON6b•ON8** and **ON6b-Pd•ON8** were sigmoidal (**Figure 11**) with  $T_m$  values of  $71.1 \pm 0.4$ ,  $66.7 \pm 0.2$  and  $65.4 \pm 0.6$  °C, respectively. In other words, both the 5'-cyclopalladated oligonucleotide as well as its unmetallated counterpart hybridized weaker than the positive control. This result was in apparent conflict with those obtained on the shorter duplexes **ON1b•ON5gag** and **ON1b-Pd•ON5gag**. Affinity of the phosphorothioate backbone for Pd(II) could explain the difference between **ON6b-Pd•ON8** and **ON6b•ON8** but not the much larger difference between **ON6•ON8** and **ON6b•ON8** or **ON6b-Pd•ON8**. We repeated the experiments with a DNA target to evaluate the different steric requirements of RNA-RNA and RNA-DNA double helices. Melting temperatures of duplexes formed by oligonucleotides **ON6**, **ON6b** and **ON6b-Pd** with **ON9** (the DNA analogue of **ON8**) were measured. Sigmoidal melting profiles were obtained producing a similar trend between **ON6**, **ON6b** and **ON6b-Pd** (**Figure 11**) but with considerably lower  $T_m$  values ( $52.4 \pm 0.9$ ,  $45.8 \pm 0.6$  and  $44.3 \pm 0.8$  °C, respectively). The reason behind the conflicting results between the short and the long duplexes remained, hence, elusive but the different target sites might offer an explanation. The 3'-overhang serving as the target site for Pd(II) coordination was the trinucleotide TCG in the short duplexes but only a single U residue in the long ones. The diethylene glycol spacer could well allow interaction of the conjugate group (benzylamine or its palladacycle) further away from the duplex than just the first unpaired residue. In any case, all the duplexes (**ON6•ON8**, **ON6b•ON8**, **ON6b-Pd•ON8**, **ON6•ON9**, **ON6b•ON9** and **ON6b-Pd•ON9**) were

deemed sufficiently stable under physiological conditions. Negative controls **ON7**, **ON7b** and **ON7b-Pd** did not form a stable duplex with the target RNA.

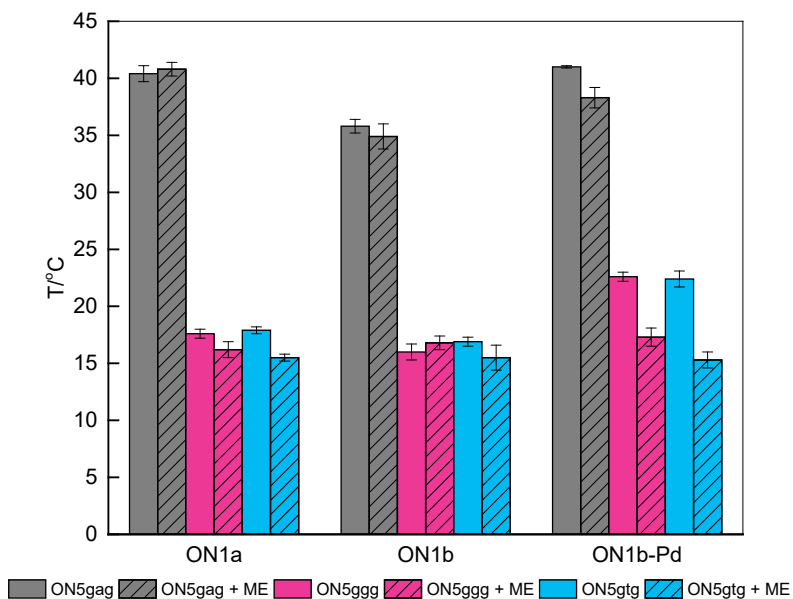


**Figure 10.** Melting temperatures of duplexes formed between **ON5gag**, **ON5ggg** and **ON5gtg** and **ON1a**, **ON1b**, and **ON1b-Pd**. Hashed bars represents experiments after addition of 100  $\mu$ M 2-mercaptoethanol.

**Table 5.** UV Melting temperatures ( $^{\circ}$ C) of duplexes formed by **ON6-ON8**, **ON6b-ON8**, **ON6b-Pd-ON8**, **ON6-ON9**, **ON6b-ON9** and **ON6b-Pd-ON9**; pH = 7.4 (20 mM cacodylate buffer); [oligonucleotides] = 3.0  $\mu$ M;  $I(\text{NaClO}_4)$  = 0.10 M.

	ON6	ON6b	ON6b-Pd
ON8	71.1 $\pm$ 0.4	66.7 $\pm$ 0.2	65.4 $\pm$ 0.6
ON9	52.4 $\pm$ 0.9	45.8 $\pm$ 0.6	44.3 $\pm$ 0.8

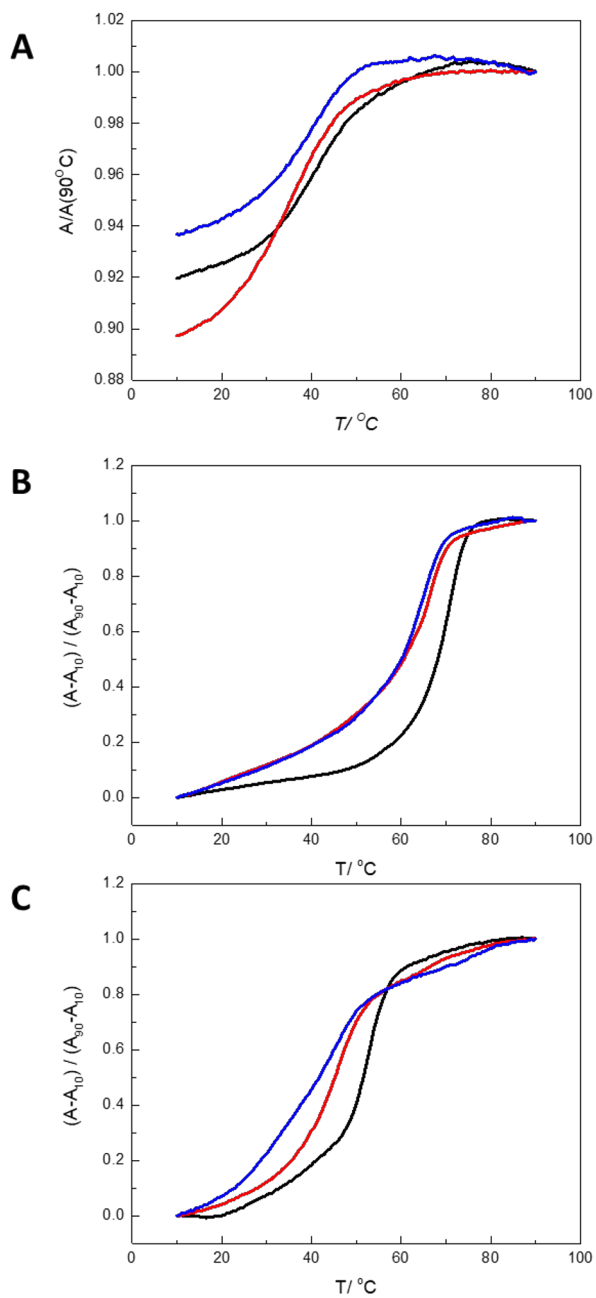


**Figure 11.** Duplexes formed by a) **ON1a•ON5gag** (black), **ON1b•ON5gag** (red) and **ON1b-Pd•ON5gag** (blue); b) **ON6•ON8** (black), **ON6b•ON8** (red) and **ON6b-Pd•ON8** (blue); c) **ON7•ON9** (black), **ON7b•ON9** (red) and **ON7b-Pd•ON9** (blue).



**Figure 12.** Schematic representation of UV Melting experiments by mixing **ON10n** and **ON5m**. **ON10n** represents **ON10cxc**, **ON10cxc-Hg**, **ON10cyc**, **ON10cyc-Pd**, **ON10czc** and **ON10czc-Pd**. **ON5m** represents **ON5gag**, **ON5gcg**, **ON5ggg** and **ON5gtg**. • represents Watson—Crick base pairing.

The flexible diethylene glycol linker between the cyclopalladated benzylamine and the oligonucleotide presumably allows the putative Pd(II) complex formed to adopt a favorable conformation. A preorganized rigid linker of the correct geometry would, however, be expected to afford even higher affinity. For better understanding of this point, hybridization affinities of oligonucleotides incorporating central isomeric *C*-nucleosides with either rigid or flexible benzaldoxime as the base moiety were determined. In this assay, modified metallated and unmetallated nucleobases were placed opposite to adenine, guanine, cytosine and thymine to test their selectivity. Accordingly, each modified oligonucleotide (**ON10cxc**, **ON10cxc-Hg**, **ON10cyc**, **ON10cyc-Pd**, **ON10czc** and **ON10czc-Pd**) was hybridized with each of the unmodified counterparts (**ON5gag**, **ON5gcg**, **ON5ggg** and **ON5gtg**). **Figure 12** presents a summary of these experiments. **Figure 13** presents the denaturation profiles of **ON10cxc•ON5gtg**, **ON10cxc-Hg•ON5gtg**, **ON10cyc•ON5gtg**, **ON10cyc-Pd•ON5gtg**, **ON10czc•ON5gtg** and **ON10czc-Pd•ON5gtg** as illustrative examples. Faster and slower eluting isomers of **ON10cxc** were studied separately. Melting temperatures of all duplexes are summarised in **Table 6**.

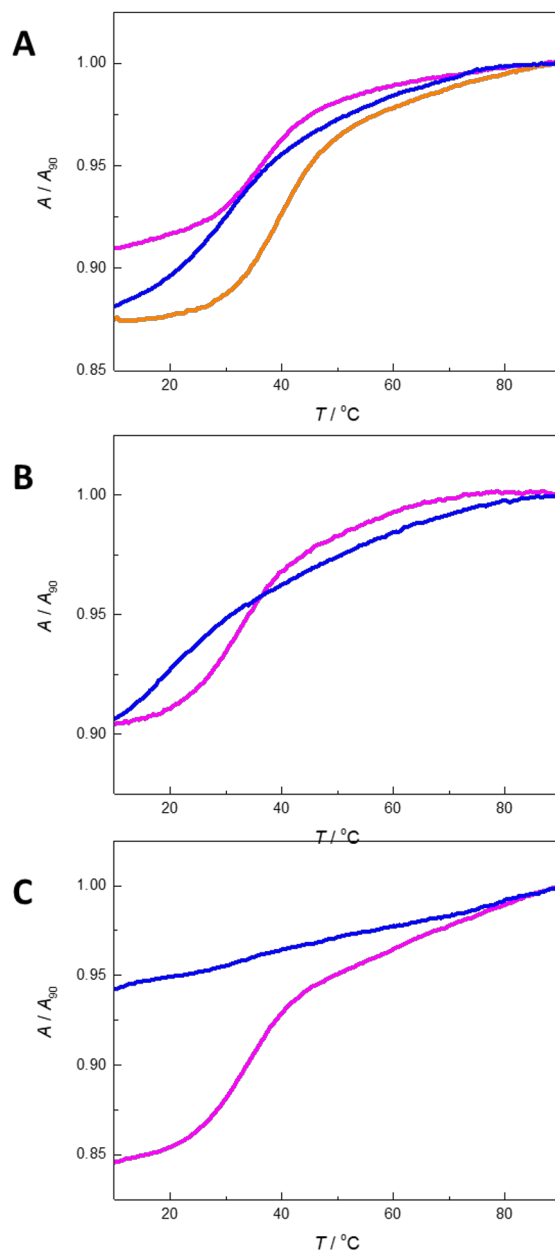


**Figure 13.** Melting profile of duplexes formed between A) **ON10cxc-ON5gtg** (magenta-faster), **ON10cxc-ON5gtg** (orange-slower), **ON10cxc-Hg-ON5gtg** (blue); B) **ON10cyc-ON5gtg** (magenta), **ON10cyc-Pd-ON5gtg** (blue); C) **ON10czc-ON5gtg** (magenta), **ON10czc-Pd-ON5gtg** (blue); pH 7.4 (20 mM cacodylate buffer); [oligonucleotides] = 1.0  $\mu\text{M}$ ;  $I(\text{NaClO}_4)$  = 0.10 M.

All metallated and unmetallated duplexes formed by **ON5gtg** exhibited sigmoidal melting profiles except duplex **ON10czc-Pd•ON5gtg** (Figure 13). Thermal stability of all of the unmetallated oligonucleotides was higher than that of their metallated counterparts except for **ON10czc-Pd**, in which case no sigmoidal profile was obtained. Duplexes formed by the slower eluting isomer of **ON10cxc** were 4-6 °C more stable than the corresponding duplexes formed by the faster eluting isomers. The highest thermal stability was observed in duplex **ON10cxc•ON5gcg** (slower eluting). The melting temperatures of duplexes formed by **ON10cxc-Hg**, in turn, were considerably lower than those of the duplexes formed by the slower eluting isomer of **ON10cxc**. Destabilization relative to the faster eluting isomer of **ON10cxc** was less pronounced but still significant.

**Table 6.** UV melting temperatures of duplexes (°C) formed by **ON10cxc**, **ON10cxc-Hg**, **ON10cyc**, **ON10cyc-Pd**, **ON10czc** and **ON10czc-Pd** with **ON5gag**, **ON5gcg**, **ON5ggg** and **ON5gtg**; pH = 7.4 (20 mM cacodylate buffer); [oligonucleotides] = 3.0 μM; I(NaClO<sub>4</sub>) = 0.10 M.

	<b>ON5gag</b>	<b>ON5gcg</b>	<b>ON5ggg</b>	<b>ON5gtg</b>
<b>ON10cxc</b> Faster	36.4 ± 0.7	33.9 ± 0.6	36.3 ± 0.7	35.4 ± 0.7
Eluting Isomer				
<b>ON10cxc</b> Slower	40.9 ± 0.5	39.6 ± 0.4	40.6 ± 0.2	39.4 ± 0.6
Eluting Isomer				
<b>ON10cxc-Hg</b>	30.9 ± 0.8	31.9 ± 0.9	31.6 ± 0.6	32.3 ± 0.8
<b>ON10cyc</b>	34.9 ± 0.5	32.2 ± 0.2	36.3 ± 0.4	32.4 ± 0.9
<b>ON10cyc-Pd</b>	18.0 ± 0.7	15.9 ± 0.9	n.a. <sup>1</sup>	17.0 ± 1.0
<b>ON10czc</b>	34.4 ± 0.8	35.0 ± 0.2	33.3 ± 0.9	34.0 ± 0.6
<b>ON10czc-Pd</b>	n.a. <sup>1</sup>	n.a. <sup>1</sup>	n.a. <sup>1</sup>	n.a. <sup>1</sup>
<b>ON10cpc</b>	34.9 ± 0.3	37 ± 0.5	38.2 ± 0.7	36 ± 1
<b>ON10cpc-Pd</b>	n.a. <sup>1</sup>	35.2 ± 0.9	40 ± 1	37 ± 1

<sup>1</sup> No sigmoidal profile was observed.

In the case of **ON10cyc-Pd•ON2g**, duplex formation was not observed within the measurable temperature range whereas the melting temperature significantly dropped to 18.0 ± 0.7, 15.9 ± 0.9 and 17.0 ± 1.0 °C for duplexes **ON10cyc-Pd•ON2a**, **ON10cyc-Pd•ON2c** and **ON10cyc-Pd•ON2t**, respectively. Even though  $T_m$  values were similar for both isomers of the unmetallated benzaldoxime (**ON10cyc** and **ON10czc**),  $T_m$  values of their palladacyclic counterparts differed dramatically. In fact, **ON10czc-Pd** did not form a stable duplex with any target sequence within the measurable temperature range of 10-90 °C. These results suggest that destabilization of **ON10cyc-Pd** and **ON10czc-Pd** is associated with the rigidity of palladacycle which in the case of **ON10cyc-Pd** was somewhat relieved by moving the oxime

linkage between the palladacycle and the ribose sugar. **ON10czc-Pd**, on the other hand, has a more rigid structure that did not allow Pd(II) mediated base pairing to opposite nucleobase.



**Figure 14.** Schematic representation of UV Melting experiments by mixing **ON10n** and **ON5m**. **ON10n** represents **ON10pcc-Pd** and **ON10ccp-Pd**, **ON10pcc** and **ON10ccp**. **ON5m** represents **ON5gga**, **ON5ggc**, **ON5ggg** and **ON5ggt**. • represents Watson—Crick base pairing.

Besides the structure of the nucleoside analogue itself, its position within the oligonucleotide sequence also affects the steric requirements and, hence, affinity and selectivity of base pairing. For example, terminal base pairs are weaker than those within the base stack and replacing them with stronger analogues can stabilize the duplex significantly. On the other hand, discrimination between base pairing partners is expected to be more rigorous within the base stack as the requirement for planarity of the base pair is more stringent. The extent to which these general observations are applicable to Pd(II)-mediated base pairing was explored with the previously reported 2-phenylpyridine *C*-nucleoside and its corresponding palladacycle as the modified residue. The modification was incorporated at either the 5'- or 3'- end of an 11-mer oligonucleotide, affording **ON10pcc** and **ON10ccp**, respectively. The corresponding palladacyclic oligonucleotides **ON10pcc-Pd** and **ON10ccp-Pd** were prepared in a similar fashion as previously reported for an oligonucleotide incorporating the same modification in the middle of the sequence.<sup>99</sup> As discussed above with the benzaldoxime oligonucleotides, the phenylpyridine oligonucleotides were also hybridized with natural oligonucleotides pairing the modified residue with a varying canonical nucleobase. The unpalladated duplexes, formed by **ON10pcc** and **ON10ccp**, produced a monophasic sigmoidal melting profile. **Figure 14** presents a summary of these experiments. Denaturation of duplexes modified at the 5'-end (**ON10pcc•ON5gga**, **ON10pcc•ON5ggc**, **ON10pcc•ON5ggg** and **ON10pcc•ON5ggt**) occurred over a range of 53-56 °C. On the other hand, when the phenylpyridine residue was placed at the 3'-end, the resulting duplexes (**ON10ccp•ON5agg**, **ON10ccp•ON5cgg**, **ON10ccp•ON5ggg** and **ON10ccp•ON5tgg**) were less stable, the  $T_m$  ranging from 48 to 51 °C.



**Table 7.** UV melting temperatures ( $^{\circ}\text{C}$ ) of duplexes formed by **ON10pcc** and **ON10pcc-Pd** with **ON5gga**, **ON5ggc**, **ON5ggg** and **ON5ggt**; pH = 7.4 (20 mM cacodylate buffer); [oligonucleotides] = 3.0  $\mu\text{M}$ ;  $I(\text{NaClO}_4)$  = 0.10 M. “Low” and “high” notations represent lower and higher melting temperatures in the case of biphasic melting curves.

	<b>ON5gga</b>	<b>ON5ggc</b>	<b>ON5ggg</b>	<b>ON5ggt</b>
<b>ON10pcc</b>	55.5 $\pm$ 0.2	53.9 $\pm$ 0.1	55.7 $\pm$ 0.1	54.2 $\pm$ 0.1
<b>ON10pcc-Pd (Low)</b>	42.0 $\pm$ 0.1	44.5 $\pm$ 0.1	40.9 $\pm$ 0.1	34.9 $\pm$ 0.1
<b>ON10pcc-Pd (High)</b>	73.0 $\pm$ 1.0	74.2 $\pm$ 0.4	67.8 $\pm$ 0.1	65.4 $\pm$ 0.1

Interestingly, denaturation of the palladated duplexes formed by **ON10pcc-Pd** and **ON10ccp-Pd** showed a biphasic melting profile with two melting temperatures. Out of the two melting temperatures of duplexes formed by **ON10pcc-Pd**, one was higher and the other one lower than the melting temperature of the respective unpalladated duplex. A similar pattern was observed in the case of duplexes formed by **ON10ccp-Pd**, except for **ON10ccp-Pd•ON5cgg**, in which case the opposite was true. Since the Pd(II) mediated base pair formation takes place at either terminus of the duplex, dissociation of all Watson—Crick base pairs followed by dissociation of the single Pd(II) mediated base pair separately seems possible. Hence, the lower melting temperatures, associated with large thermal hyperchromicity, were assigned to Watson—Crick melting. In this context, it is interesting to note that the UV melting profiles reported previously for duplexes incorporating a central cyclopalladated phenylpyridine residue were monophasic, with melting temperatures similar to the “low” melting temperatures of the terminally modified duplexes. The favoured base pairing partner was also different: cytosine in the case of a terminal and guanine in the case of a central palladacyclic residue. These results clearly show that the position of the modified nucleobase in the sequence affects not only the choice of the base pairing partner but also the duplex stability.

**Table 8.** UV melting temperatures ( $^{\circ}\text{C}$ ) of duplexes formed by **ON10ccp** and **ON10ccp-Pd** with **ON5agg**, **ON5cgg**, **ON5ggg** and **ON5tgg**; pH = 7.4 (20 mM cacodylate buffer); [oligonucleotides] = 3.0  $\mu\text{M}$ ;  $I(\text{NaClO}_4)$  = 0.10 M. “Low” and “high” notations represents lower and higher melting temperatures in the case of biphasic melting curves.

	<b>ON5agg</b>	<b>ON5cgg</b>	<b>ON5ggg</b>	<b>ON5tgg</b>
<b>ON10ccp</b>	50.7 $\pm$ 0.1	50.9 $\pm$ 0.1	48.6 $\pm$ 0.1	49.8 $\pm$ 0.1
<b>ON10ccp-Pd (low)</b>	42.3 $\pm$ 0.3	56.4 $\pm$ 0.2	44.3 $\pm$ 0.2	48.9 $\pm$ 0.1
<b>ON10ccp-Pd (high)</b>	67.1 $\pm$ 0.2	77.5 $\pm$ 0.1	71.6 $\pm$ 0.3	71.5 $\pm$ 0.1

### 3.3 CD Melting studies of cyclopalladated, mercurated and unmetallated oligonucleotides

Secondary structures of all modified (metallated and unmetallated) duplexes were determined by obtaining temperature dependent circular dichroism (CD) spectra. CD spectra, recorded at 10 °C intervals for all duplexes, exhibited a negative Cotton effect between 240 and 260 nm and a positive Cotton effect between 270 and 280 nm, consistent with right-handed B-type double helical DNA structures. Intensity of the positive and negative bands was almost similar. At higher temperatures, the signals diminished signifying unwinding of duplexes. Representative CD melting profiles of duplexes formed by oligonucleotides bearing a palladacyclic residue either at the 5'- terminus (**ON1b-Pd•ON5gag**) or in the middle of the sequence (**ON10cyc-Pd•ON5gtg**) are shown in **Figure 15**.

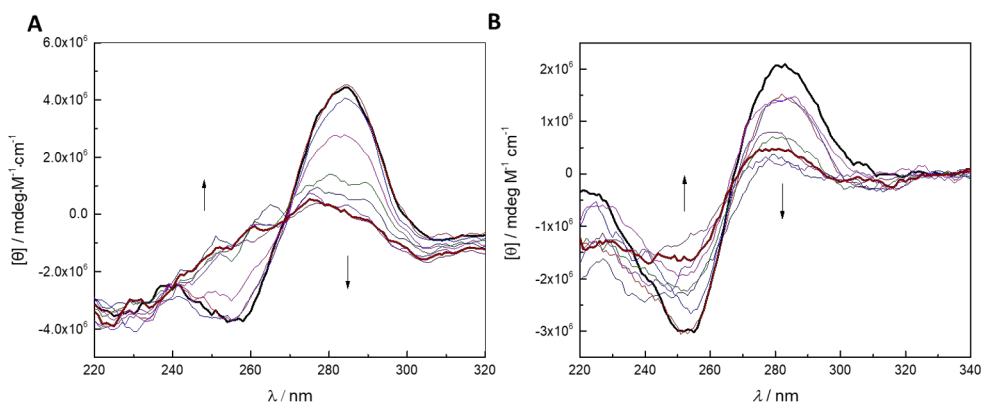


**Figure 15.** CD spectra of A) **ON1b-Pd•ON5gag** ([oligonucleotides] = 3.0  $\mu$ M) and B) **ON10cyc-Pd•ON5gtg** ([oligonucleotides] = 1.0  $\mu$ M) recorded at 10 °C intervals between 10 and 90 °C; pH = 7.4 (20 mM cacodylate buffer);  $I(\text{NaClO}_4)$  = 0.10 M. Spectra acquired at extreme temperatures are indicated by thicker lines and thermal shifts of the minima and maxima by arrows.

Naturally, the shorter oligonucleotides **ON2b-Pd**, **ON3b-Pd** and **ON4b-Pd**, as well as their unmetallated analogues, gave weak CD signals reflecting their inability of forming duplexes above 10 °C. Similarly, spectra of **ON10cyc-Pd** with all unmodified oligonucleotides (**ON5gag**, **ON5geg**, **ON5ggg** and **ON5gtg**) were distorted with low ellipticity indicating no duplex formation between 10 and 90 °C. Remarkably, CD spectra of duplexes formed by the 5'-modified 2-phenylpyridine oligonucleotide **ON10pcc** and its palladacyclic counterpart **ON10pcc-Pd** exhibited an additional positive Cotton effect between 280 and 290 nm.

### 3.4 Thermodynamic Analysis of Melting Curves

Besides the melting temperature, careful analysis of melting curves offers more information about the enthalpy ( $\Delta H^\circ$ ) and entropy ( $\Delta S^\circ$ ) of hybridization. Watson—Crick hydrogen bonding as well as base stacking are associated with unfavorable (i.e. negative) entropy and favorable (i.e. also negative) enthalpy of the system. When metal coordination is involved the situation is more complicated as the entropic penalty of base pairing may to some extent be offset by the positive entropy of desolvation of the metal center. Enthalpies ( $\Delta H^\circ$ , **Table 9**) and entropies ( $\Delta S^\circ$ , **Table 10**) of hybridization were determined for duplexes formed by **ON1a**, **ON1b**, **ON1b-Pd**, **ON10cxc**, **ON10cxc-Hg**, **ON10cyc**, **ON10cyc-Pd**, **ON10czc** and **ON10czc-Pd** as described previously.<sup>100</sup>

Structural rigidity of the palladacyclic benzaldoxime nucleobases had a major impact on the stability of the respective double-helical oligonucleotides. Despite of being structural isomers of each other, **ON10cyc-Pd** and **ON10czc-Pd** demonstrated a huge difference in Pd(II) mediated base pairing by  $T_m$  measurements. Moreover, duplexes formed by **ON10cxc-Hg**, **ON10cyc-Pd** and **ON10czc-Pd** were less stable than duplexes formed by the unmetallated analogues **ON10cxc**, **ON10cyc** and **ON10czc**. Thermodynamic analysis of the UV melting curves provided additional insight into the Pd(II) and Hg(II) mediated base pairing within these duplexes.

**Table 9.** Enthalpies of hybridization ( $\Delta H^\circ$  / kJ mol<sup>-1</sup>) for duplex formed by the modified oligonucleotides **ON1a**, **ON1b**, **ON1b-Pd**, **ON10cxc**, **ON10cxc-Hg**, **ON10cyc**, **ON10cyc-Pd**, **ON10czc** and **ON10czc-Pd** and unmodified oligonucleotides **ON5a**, **ON2a**, **ON2c**, **ON2g** and **ON2t**; pH 7.4 (20 mM cacodylate buffer); [oligonucleotides] = 1.0 or 3.0  $\mu$ M;  $I(\text{NaClO}_4) = 0.10$  M.

	<b>ON5a</b>	<b>ON2a</b>	<b>ON2c</b>	<b>ON2g</b>	<b>ON2t</b>
<b>ON1a</b>	-200 $\pm$ 20	n.a. <sup>1</sup>	n.a. <sup>1</sup>	n.a. <sup>1</sup>	n.a. <sup>1</sup>
<b>ON1b</b>	-200 $\pm$ 10	n.a. <sup>1</sup>	n.a. <sup>1</sup>	n.a. <sup>1</sup>	n.a. <sup>1</sup>
<b>ON1b-Pd</b>	-250 $\pm$ 20	n.a. <sup>1</sup>	n.a. <sup>1</sup>	n.a. <sup>1</sup>	n.a. <sup>1</sup>
<b>ON10cxc</b> <sup>[a]</sup>	n.a. <sup>1</sup>	-279 $\pm$ 3	-259 $\pm$ 2	-252 $\pm$ 2	-285 $\pm$ 4
<b>ON10cxc</b> <sup>[b]</sup>	n.a. <sup>1</sup>	-259 $\pm$ 1	-296 $\pm$ 3	-277 $\pm$ 1	-278 $\pm$ 2
<b>ON10cxc-Hg</b>	n.a. <sup>1</sup>	-219 $\pm$ 1	-183 $\pm$ 3	-234 $\pm$ 4	-239 $\pm$ 3
<b>ON10cyc</b>	n.a. <sup>1</sup>	-286 $\pm$ 3	-278 $\pm$ 3	-304 $\pm$ 5	-320 $\pm$ 6
<b>ON10cyc-Pd</b>	n.a. <sup>1</sup>	-166 $\pm$ 2	-109 $\pm$ 2	n.a. <sup>2</sup>	-177 $\pm$ 4
<b>ON10czc</b>	n.a. <sup>1</sup>	-336 $\pm$ 5	-270 $\pm$ 10	-232 $\pm$ 3	-285 $\pm$ 3
<b>ON10czc-Pd</b>	n.a. <sup>1</sup>	n.a. <sup>2</sup>	n.a. <sup>2</sup>	n.a. <sup>2</sup>	n.a. <sup>2</sup>

<sup>1</sup> Experiment was not carried out. <sup>2</sup>No sigmoidal curve was obtained. <sup>[a]</sup> Faster-eluting isomer. <sup>[b]</sup> Slower-eluting isomer.

No clear pattern of more negative enthalpies and entropies of hybridization of the isomers of **ON10cxc** emerged, leaving the reason behind the different  $T_m$  values obscure. Duplexes formed by **ON10cxc-Hg** had a lower entropy of hybridization

(500-600 J mol<sup>-1</sup> K<sup>-1</sup>) than those formed by **ON10cxc** (700-800 J mol<sup>-1</sup> K<sup>-1</sup>), but still considerably higher than previously reported for other Hg(II) mediated duplexes (200-400 J mol<sup>-1</sup> K<sup>-1</sup>)<sup>101</sup>. Hg(II) mediated base pairing takes place with concomitant dehydration of the Hg(II) ion that contributes positively to entropy.<sup>101,102,103</sup> However, restricted  $\sigma$  bond rotations could largely nullify this effect in the case of **ON10cxc-Hg**. On other hand, duplexes formed by **ON10cxc-Hg** and duplexes formed by 5-mercuricytosine modified oligonucleotides were comparable in terms of enthalpies of hybridization. (**Table 10**)

**Table 10.** Entropies of hybridization ( $\Delta S^\circ/\text{J}\cdot\text{mol}^{-1}\cdot\text{K}^{-1}$ ) for duplex formed by the modified oligonucleotides **ON1a**, **ON1b**, **ON1b-Pd**, **ON10cxc**, **ON10cxc-Hg**, **ON10cyc**, **ON10cyc-Pd**, **ON10czc** and **ON10czc-Pd** and unmodified oligonucleotides **ON5a**, **ON2a**, **ON2c**, **ON2g** and **ON2t**; pH 7.4 (20mM cacodylate buffer); [oligonucleotides]= 1.0 or 3.0  $\mu\text{M}$ ; I(NaClO<sub>4</sub>)=0.10 M.

	<b>ON5a</b>	<b>ON2a</b>	<b>ON2c</b>	<b>ON2g</b>	<b>ON2t</b>
<b>ON1a</b>	-530 ± 50	n.a. <sup>1</sup>	n.a. <sup>1</sup>	n.a. <sup>1</sup>	n.a. <sup>1</sup>
<b>ON1b</b>	-550 ± 40	n.a. <sup>1</sup>	n.a. <sup>1</sup>	n.a. <sup>1</sup>	n.a. <sup>1</sup>
<b>ON1b-Pd</b>	-670 ± 50	n.a. <sup>1</sup>	n.a. <sup>1</sup>	n.a. <sup>1</sup>	n.a. <sup>1</sup>
<b>ON10cxc</b> <sup>[a]</sup>	n.a. <sup>1</sup>	-774 ± 9	-725 ± 06	-639 ± 6	-800 ± 10
<b>ON10cxc</b> <sup>[b]</sup>	n.a. <sup>1</sup>	-708 ± 2	-820 ± 10	-762 ± 4	-770 ± 04
<b>ON10cxc-Hg</b>	n.a. <sup>1</sup>	-591 ± 6	-486 ± 08	-640 ± 10	-660 ± 10
<b>ON10cyc</b>	n.a. <sup>1</sup>	-815 ± 8	-794 ± 08	-870 ± 20	-930 ± 20
<b>ON10cyc-Pd</b>	n.a. <sup>1</sup>	-445 ± 5	-259 ± 06	n.a. <sup>2</sup>	-480 ± 10
<b>ON10czc</b>	n.a. <sup>1</sup>	-980 ± 20	-770 ± 30	-638 ± 8	-808 ± 70
<b>ON10czc-Pd</b>	n.a. <sup>1</sup>	n.a. <sup>2</sup>	n.a. <sup>2</sup>	n.a. <sup>2</sup>	n.a. <sup>2</sup>

<sup>1</sup> Experiment was not carried out. <sup>2</sup> No sigmoidal curve was obtained. <sup>[a]</sup> Faster-eluting isomer. <sup>[b]</sup> Slower-eluting isomer.

Pd(II) coordination of the 5'-terminal benzylamine palladacycle of **ON1b-Pd** to the opposite strand appears to be an enthalpy-driven process, whereas the entropic penalty is consistent with restricted conformation of the flexible linker. The net effect is stabilizing, as evidenced by the fact that Pd(II) mediated interaction between **ON1b-Pd** and **ON5a** promoted hybridization more than Watson—Crick hydrogen bonding between **ON1b** and **ON5a**. On the other hand, in the case of **ON10cyc-Pd**, containing a central benzaldoxime palladacycle, enthalpies and entropies of hybridization were less negative than with **ON10cyc**. This result, while at first glance in conflict with those obtained with **ON1b-Pd**, can be understood if hybridization of **ON10cyc-Pd** with the complementary strand is incomplete even at 10 °C (as the UV melting profile in **Figure 13B** would seem to suggest).

### 3.5 Fluorescence Studies of cyclopalladated and unpalladated oligonucleotides

Previous results of UV melting experiments obtained for **ON10cpc-Pd** suggested highly stable central Pd(II) mediated base pairing with canonical nucleobases.<sup>94</sup> Moreover, biphasic melting profiles of duplexes formed by **ON10pcc-Pd** and **ON10ccp-Pd** suggest the persistence of terminal Pd(II) mediated base pairs at high temperature. A fluorescence based strand displacement assay was designed to complement those results. While in a UV melting study a stable Pd(II)-mediated base pair with a geometry incompatible with the geometry of a double helix would result in a low observed melting temperature, the same base pair could still be effective in promoting strand displacement.<sup>97</sup>

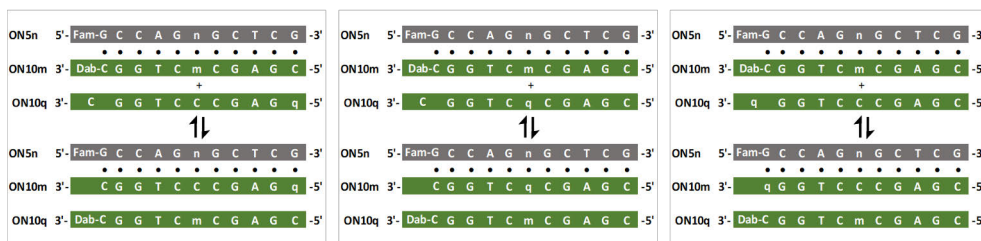


**Figure 16.** Schematic representation of FRET experiments by mixing duplex **ON5n•ON10m** with **ON10q**. **ON10m•ON5n** represents duplexes **ON10ctc-Dabcyl•ON5gag-Fam**, **ON10cgc-Dabcyl•ON5gcg-Fam**, **ON10ccc-Dabcyl•ON5ggg-Fam**, and **ON10cac-Dabcyl•ON5gtg-Fam**. **ON10q** represents **ON10pcc-Pd**, **ON10cpc-Pd**, **ON10ccp-Pd**, **ON10pcc**, **ON10cpc**, and **ON10ccp**. • represents Watson—Crick base pairing.

A Förster Resonance Energy Transfer (FRET) based competition assay was carried out to assess the binding preferences by determining the strand displacement ability of cyclopalladated oligonucleotides **ON10pcc-Pd**, **ON10cpc-Pd**, **ON10ccp-Pd** and their unmetallated counterparts in target duplexes. Terminal modifications in **ON10pcc-Pd** and **ON10ccp-Pd** allowed to determine fidelity of Watson—Crick base pairing away from the putative Pd(II) mediated base pairs, similarly to the duplexes formed by **ON1b-Pd**, while with **ON10cpc-Pd** selectivity of the Pd(II) mediated base pairing itself was of interest. Four fully matched target duplexes (**ON10ctc-Dabcyl•ON5gag-Fam**, **ON10cgc-Dabcyl•ON5gcg-Fam**, **ON10ccc-Dabcyl•ON5ggg-Fam**, **ON10cac-Dabcyl•ON5gtg-Fam**) were employed, one strand bearing a fluorophore (6-Carboxyfluorescein, Fam) at the 5'- terminus and another a quencher ({{[4-(dimethylamino)phenyl]azo}benzoic acid, Dabcyl) at the 3'- terminus. **Figure 16** presents a summary of these experiments. At 10 °C, the target duplexes were fully hybridized and hence the fluorophore and the quencher of the FRET pair in close proximity to each other, resulting in weak emission. At 90

°C, the target duplexes were strongly emissive which is consistent with unwinding of the duplex resulting in dissociation of the FRET pair. Fluorescence emission spectra on excitation at 493 nm were acquired at 10 °C and 90 °C, showing a single maximum at 525 nm. Intensities recorded at 10 °C and 90 °C were taken as references representing fully hybridized and dissociated forms, respectively.

Except for the modified residue, the cyclopalladated oligonucleotides had the same sequence as one of the quencher oligonucleotides (**ON10ccc-DabcyI**). Therefore, addition of either the cyclopalladated oligonucleotides or their unmetallated counterparts can displace the quencher strand and form a double helical structure with the fluorophore bearing strand. This association and concomitant dissociation of the FRET pair was quantified based on fluorescence emission intensity by following equation.<sup>97</sup>

$$\% \text{ displacement} = \frac{\text{intensity (mixture at } 10^{\circ}\text{C)} - \text{intensity (target duplex at } 10^{\circ}\text{C)}}{\text{intensity (target duplex at } 90^{\circ}\text{C)} - \text{intensity (target duplex at } 10^{\circ}\text{C)}}$$

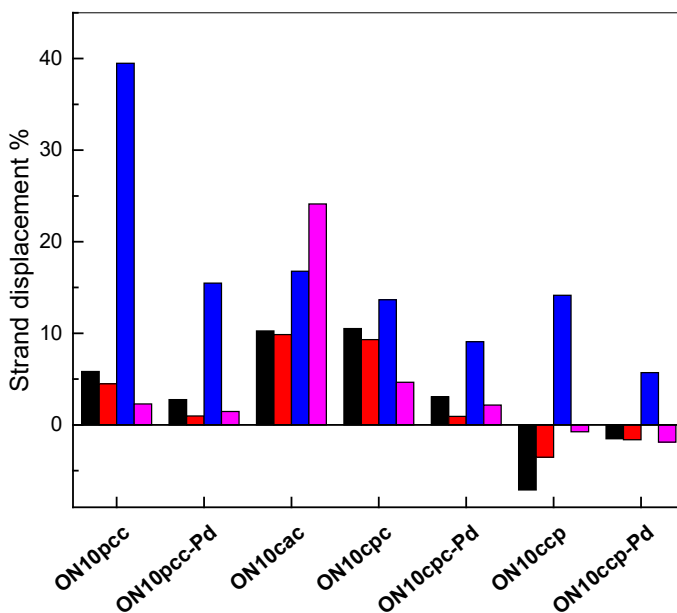


**Figure 17.** Strand displacement from duplexes **ON10ctc-DabcyI-ON5gag-Fam** (black), **ON10cgc-DabcyI-ON5gcg-Fam** (red), **ON10ccc-DabcyI-ON5ggg-Fam** (blue), **ON10cac-DabcyI-ON5gtg-Fam** (magenta) by various modified and natural oligonucleotides;  $T = 10^{\circ}\text{C}$ ;  $\text{pH} = 7.4$  (20 mM cacodylate buffer);  $[\text{oligonucleotides}] = 50 \text{ nM}$ ;  $I(\text{NaClO}_4) = 0.10 \text{ M}$ .

Competition was first explored by mixing the natural oligonucleotide **ON10cac** with target the duplex **ON10cac-Dabcyl•ON1gtg-Fam** where **ON10cac** has the same sequence as the quencher oligonucleotide. The mixture was annealed at 90 °C followed by gradual cooling to 10 °C before measurement at 10 °C. If **ON10cac** is able to displace **ON10cac-Dabcyl**, fluorescence emission intensity is expected to increase to 50% of the maximum intensity attained at high temperature, representing a state where 50% of **ON1gtg-Fam** is hybridized with **ON10cac-Dabcyl** and 50% with **ON10cac**, provided that the FRET pair itself has no impact on duplex stability. The observed displacement of **ON10cac-Dabcyl** from the fully matched duplex **ON10cac-Dabcyl•ON1gtg-Fam** by **ON10cac** was only 21% which suggests favorable interaction between Fam and Dabcyl at low temperature. As expected, the displacement ability of **ON10cac** was consistently lower when the resulting duplex contained a mismatch.

Displacement of the quencher strand from the various target duplexes after mixing with a modified oligonucleotide is summarized in **Figure 17**. Dissociation of the FRET pair within **ON10ccc-Dabcyl•ON1ggg-Fam** by each of the three palladated oligonucleotides allows one to determine the sequence dependence of Pd(II) mediated base pairing. Guanine appeared to be the best base pairing partner irrespective of the position of the 2-phenylpyridine residue in **ON10pcc**, **ON10cpc** and **ON10ccp**. In other words, displacement of **ON10ccc-Dabcyl** was more favorable compared to the other quencher strands (**ON10cac-Dabcyl**, **ON10cgc-Dabcyl** and **ON10ctc-Dabcyl**). In the case of respective cyclopalladated oligonucleotides, guanine remained the best base pairing partner, however, the displacement ability significantly dropped when 2-phenylpyridine was replaced by its palladacyclic derivative. Preference for guanine as the Pd(II) mediated base pairing partner was consistent with the results of the UV melting temperature experiments on **ON10cpc-Pd**. Among the palladated oligonucleotides, **ON10pcc-Pd** was the most efficient to displace the quencher strand from **ON10ccc-Dabcyl•ON1ggg-Fam**, followed by **ON10cpc-Pd** and **ON10ccp-Pd**. In other words, Pd(II) mediated base pairing between 2-phenylpyridine and guanine is tolerated best at the 5'-terminus and worst at the 3'-terminus. These results further underline the significance of the position of the modified nucleobase in an oligonucleotide.

### 3.6 Splice-Correction

As a first demonstration of applicability to a biological system, phosphorothioate oligonucleotides having either cyclopalladated or unpalladated benzylamine incorporated at the 5'-terminus through a flexible linker were tested for their splice correction ability. Three reporter cell lines, human cervical cancer (HeLa Luc/705),

human osteosarcoma (U-2 OS\_705) and human liver (HuH7\_705) were used. These reporter cell lines carried a mutated  $\beta$ -globin intron 2 interrupted pLuc/705 splice-switching reporter gene.<sup>104,105,106</sup> The mutated intron presents an aberrant 5' splice site that activates a cryptic 3' splice site, and results in the translation of non-functional luciferase.<sup>105</sup> With each cell line, the oligonucleotides were delivered either with Lipofectamine 2000 or by gymnosis without any transfecting reagent.

With both delivery methods, each of the three reporter cell lines was transfected with either the 5'-cyclopalladated benzylamine modified oligonucleotide **ON6b-Pd**, its unmetallated counterpart **ON6b** or the positive control **ON6**. These modified oligonucleotides had a sequence complementary to the aberrant splice site. Hybridization of the complementary oligonucleotide with the aberrant splice site would be expected to result in splice-correction, which yields correct mRNA and thus restores luciferase activity. Non-complementary sequences **ON7**, **ON7b** and **ON7b-Pd** were used as negative controls. **ON7b** has been previously reported as not being able to perform splice correction.

### 3.6.1 Lipofectamine 2000 Mediated Transfection

HeLa Luc/705 cell lines were treated by modified and control oligonucleotides at three different concentrations (25 nM, 50 nM and 100 nM). **Figure 18a** presents the restoration of luciferase activity at different concentrations. Remarkable restoration of luciferase activity was observed for all complementary oligonucleotides. At all concentrations, the cyclopalladated oligonucleotide **ON6b-Pd** was the most efficient in splice correction followed by the unpalladated analogue **ON6b** and the positive control **ON6**. Except for the highest concentrations, non-complementary oligonucleotides were inactive.

HuH7\_705 and U-2 OS\_705 cell lines were transfected at a single oligonucleotide concentration of 100 nM. The restoration of luciferase activity is shown in **Figure 18 (c and d)**. Activity of **ON6** in HuH7\_705 cell line was comparable to that observed with HeLa Luc/705 cells at 100 nM concentration while a notable drop in restoration was seen in the case of U-2\_OS\_705 cells. In both of these cell lines, the positive control **ON6** was the most efficient in splice correction followed by almost equal efficiency of **ON6b** and **ON6b-Pd**. All non-complementary oligonucleotides were inactive apart from anomalous activity of **ON7b** in the HuH7\_705 cell line.



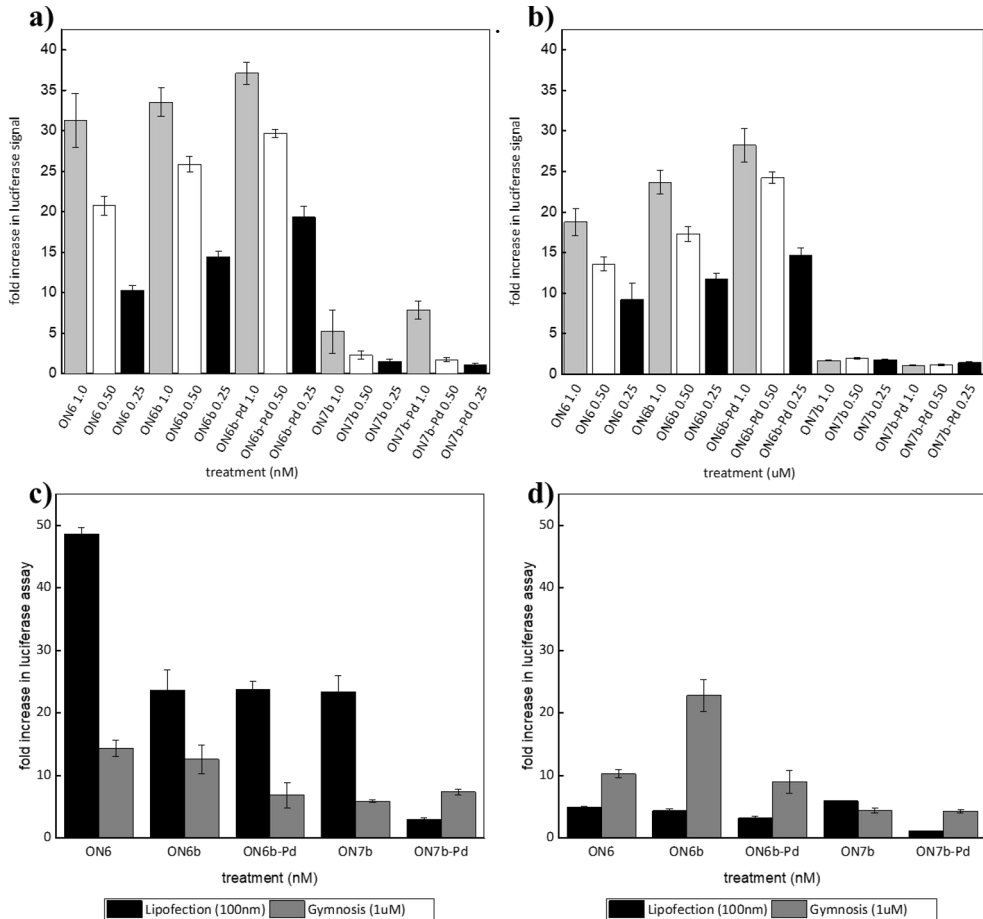


**Figure 18.** Restoration of Luciferase activity in a) HeLa Luc/705 cells by lipofection; b) HeLa Luc/705 cells by gymnosis; c) HuH7\_705 by lipofection and gymnosis; d) U-2 OS\_705 by lipofection and gymnosis

### 3.6.2 Gymnosis

Naked delivery of modified oligonucleotides to HeLa Luc/705 cell lines was carried out at three different concentrations (25 nM, 50 nM and 100 nM) presented in **Figure 18b**. HuH7\_705 and U-2 OS\_705 cell lines were treated at a single concentration of 100 nM presented in **Figure 18 (c and d)**. Except for the U-2 OS\_705 cell line, transfection by Lipofectamine resulted in more efficient splice correction than gymnosis. In the case of the HeLa Luc/705 cell line, highest restoration in luciferase activity was again observed by **ON6b-Pd**, producing a similar dose response pattern as with Lipofectamine 2000 mediated delivery. In line with lipofection mediated

delivery, positive control **ON6** was the most efficient splice correcting agent in the HuH7\_705 cell line followed by **ON6b** and **ON6b-Pd**. On the other hand, in the case of the U-2 OS\_705 cell line, **ON6b** was the most efficient, followed by **ON6** and **ON6b-Pd**.

### 3.7 Cytotoxicity Assay

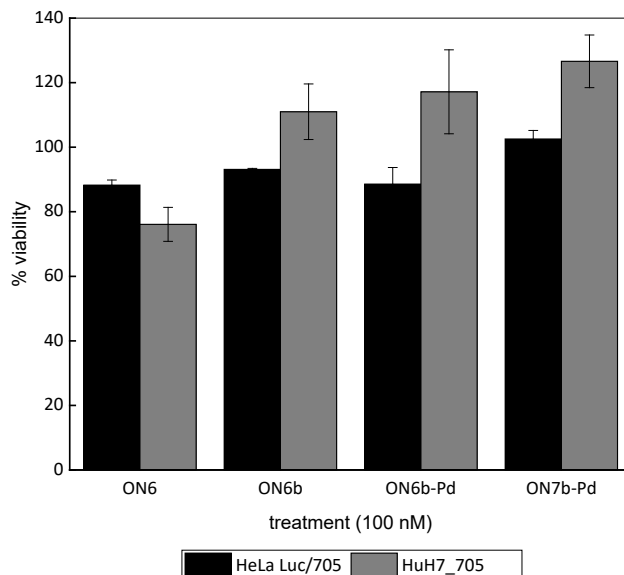


**Figure 19.** Viability of HeLa Luc/705 and HuH7\_705 cells upon lipofection. Values are expressed as the ratio of the absorbance at 450 nm of the treated cells to the untreated cells.

Post Lipofectamine 2000 mediated transfection, survival of HeLa Luc/705 and HuH7\_705 cells was evaluated by WST-1 cell proliferation assay. Both cell lines were treated with a single oligonucleotide concentration of 100 nM. Results obtained from the assay are shown in **Figure 19**. None of the oligonucleotides tested (positive control **ON6**, the 5'-modified cyclopalladated oligonucleotide **ON6b-Pd**, its unmetallated counterpart **ON6b** and the 5'-modified cyclopalladated negative control **ON7b-Pd**) exhibited significant toxicity to either cell line. With both cell lines, 5'-modified oligonucleotides were actually somewhat less toxic than their unmodified counterparts.

## 4 Conclusion

Covalently metallated oligonucleotides were prepared by two different methods. Cyclopalladated benzylamine oligonucleotides (**ON1b-Pd**, **ON2b-Pd**, **ON3b-Pd**, **ON4b-Pd**), cyclopalladated 2-phenylpyridine oligonucleotides (**ON10pcc-Pd**, **ON10ccp-Pd**) and the rigid isomer of cyclopalladated benzaldoxime oligonucleotides (**ON10czc-Pd**) were prepared by post-synthetic treatment with lithium tetrachloropalladate. The flexible isomers of either cyclopalladated or mercurated benzaldoxime oligonucleotides, in turn, were prepared by oxime coupling between aminoxy-functionalized oligonucleotides and organometallic benzaldehydes.

UV and CD melting studies revealed a clear pattern of higher duplex stability in cases where the environment of the palladacyclic residue is flexible. Accordingly, the greatest stabilization by putative Pd(II) coordination was observed with oligonucleotides having a cyclopalladated benzylamine conjugated to the 5'-terminus through a flexible diethylene glycol linker. Within the sterically more constrained environment of the base stack of the double helix, Pd(II) mediated base pairs formed by palladacyclic benzaldoxime *C*-nucleosides resulted in lower melting temperatures than those of the corresponding unmetallated duplexes. However, duplexes incorporating a flexible isomer of the benzaldoxime nucleobase were more stable than those incorporating a rigid isomer. Impact of incorporating a cyclopalladated 2-phenylpyridine *C*-nucleoside at either terminus or in the middle of the oligonucleotide on duplex stability was studied by both UV melting and FRET-based strand displacement experiments. Biphasic UV melting profiles of duplexes formed by the terminally modified oligonucleotides suggests the existence of Pd(II) mediated base pairs at temperatures higher than the Watson—Crick melting temperature of those duplexes. Based on the strand displacement experiments, a Pd(II) mediated base pair between guanine and 2-phenylpyridine was better tolerated at the 5'-terminus than at the 3'-terminus or in the middle of the duplex. Such sequence dependence, along with the requirement for flexibility, suggest that the geometries of the putative Pd(II) mediated base pairs studied so far are not entirely compatible with that of the DNA double helix.

As a demonstration of the applicability of organometallic oligonucleotides in biological systems, a phosphorothioate oligonucleotide bearing a 5'-terminal cyclopalladated benzylamine residue was tested for its splice correction ability in various human cell lines. Cyclopalladated oligonucleotides delivered using standard protocols were non-toxic to cells. Lipofection proved to be the most efficient way of transfection in HeLa Luc/705 and HuH7\_705 cell lines whereas U-2 OS\_705 cell lines responded better to naked delivery. Moreover, the modified oligonucleotides demonstrated a modestly higher splice correction efficiency in the HeLa Luc/705 cell line than the unmodified analogue. These results indicate the possibility of using cyclopalladated oligonucleotides as therapeutic agents.

# 5 Experimental

## 5.1 General Methods

All air and/or moisture sensitive experiments were carried out using oven-dried glassware under nitrogen or argon atmosphere. All solvents involved in air and/or moisture sensitive experiments were dried using 3 and 4 Å molecular sieves. The syntheses and characterization of novel compounds are described in the original publications. All novel compounds were characterized by  $^1\text{H}$ ,  $^{13}\text{C}$ ,  $^{31}\text{P}$  NMR (Bruker 500 MHz and Bruker 600 MHz Cryo) and HRMS (ESI MS-QToF) when applicable.

## 5.2 Oligonucleotide Synthesis

All oligonucleotides were synthesized at 1  $\mu\text{mol}$  scale on an Applied Biosystems 3400 automated DNA/RNA synthesizer by using conventional phosphoramidite strategy. Coupling time for modified building blocks was extended to 300 s. According to trityl response, all couplings proceeded with normal efficiency.

Support-bound **ON10c9c'** was treated with 2% dichloroacetic acid and 1%  $\text{H}_2\text{O}$  in  $\text{CH}_2\text{Cl}_2$  at 25 °C for 2 h to remove the acetal protecting group of the benzaldehyde residue. Support-bound **ON10c13c** was treated with hydrazine acetate in pyridine at 25 °C for 45 min to remove the phthaloyl protection of the aminoxy residue. The support-bound aminoxy-functionalized **ON10c13c'** was further treated with either 3-hydroxybenzaldehyde (10 mg, 82  $\mu\text{mol}$ ) in  $\text{CH}_2\text{Cl}_2$  (3.0 mL) or neat benzaldehyde (3.0 mL, 29 mmol) to afford oligonucleotides **ON10cxc-Hg** and **ON10cyc-Pd**, respectively. Finally, all oligonucleotides were released from the solid support and the phosphate and base moieties were deprotected by incubation in 25 % aqueous ammonia at 55 °C for 12 h. Purification was carried out by RP-HPLC on a Hypersil ODS C18 column (250×4.6 mm, 5  $\mu\text{m}$ ) eluting with a linear gradient (details can be found in the original publications)<sup>90</sup> of MeCN in 50 mM aqueous triethylammonium acetate. The flow rate was 1.0 mL  $\text{min}^{-1}$  and the detection wavelength 260 nm.

### 5.3 UV Melting and CD Melting Temperature Studies

Melting profiles were recorded on a PerkinElmer Lambda 35 UV-Vis spectrometer equipped with a Peltier temperature control unit using quartz cuvettes with 10 mm optical path length. Temperature was varied at a rate of 0.5 °C min<sup>-1</sup> between 10 and 90 °C.

CD spectra were recorded on an Applied Photophysics Chirascan spectropolarimeter equipped with a Peltier temperature control unit. All CD spectra were recorded over a wavelength range of 200 - 400 nm and over a temperature range of 10–90 °C, sampling at 10 °C intervals. An internal thermometer was used to confirm the accurate target temperature.

Samples used to measure UV and CD melting profiles were identical. The samples were prepared in quartz glass cuvettes of 10.00 mm optical path by mixing the appropriate oligonucleotides to a final concentration of 1.0 or 3.0 μM depending on the oligonucleotide sequences. The pH of the samples was adjusted to 7.4 with 20 mM cacodylate buffer and the ionic strength to 0.10 M with NaClO<sub>4</sub>.

### 5.4 Fluorescence Studies

Fluorescence experiments were carried out on a Cary Eclipse fluorescence spectrometer using an excitation wavelength of 493 nm. Emission wavelength range was set from 500 to 700 nm. The excitation and emission slits were set to 5 nm, the PMT voltage to 600 V and the scan rate to 120 nm min<sup>-1</sup>. The samples were prepared in quartz glass cuvettes of 10.00 mm optical path by mixing the appropriate oligonucleotides to a final concentration of 50 nM. Each of the target duplexes (**ON10ctc-Dabcyl•ON5gag-Fam**, **ON10cgc-Dabcyl•ON5gcg-Fam**, **ON10ccc-Dabcyl•ON5ggg-Fam** and **ON10cac-Dabcyl•ON5gtg-Fam**) was first annealed by heating to 90 °C and then gradually allowed to cool to 10 °C, after which the emission spectra were recorded at 10 and 90 °C. The duplex samples were then split to seven parts and an equimolar amount of one of the displacer oligonucleotides (**ON10pcc**, **ON10pcc-Pd**, **ON10cac**, **ON10cpc**, **ON10cpc-Pd**, **ON10ccp** and **ON10ccp-Pd**) was added to each. The resulting samples were then again heated to 90 °C and allowed to cool to 10 °C, at which temperature fluorescence emission spectra were recorded.

## 5.5 Biological Experiments

### 5.5.1 Cell Lines and Culture Conditions

The three reporter cell lines, HeLa Luc/705 (human cervical cancer cells), HuH7\_705 (human liver cells) and U-2 OS\_705 (human osteosarcoma cells), were cultured and maintained in high glucose Dulbecco's modified Eagle's medium (DMEM) supplemented with 10% fetal bovine serum (FBS) at 37 °C in a humidified incubator with 5% CO<sub>2</sub>.

### 5.5.2 Transfection by Lipofectamine 2000

Cells were seeded one day before transfection, at a density of  $1.1 \times 10^4$  per well in white TC-Treated 96-well plates, to reach cell confluency of approximately 70–80%. Lipofectamine 2000/oligonucleotide (25, 50 or 100 nM) complexes were prepared in OptiMEM<sup>®</sup> for transfection according to the manufacturer's protocol. Culture media were removed and 100 µL of complexes were added per well. After transfection time of 4 h, the complexes were replaced with complete media containing 10% FBS (100 µL per well). Cells were incubated for another 20 h at 37 °C in a humidified incubator with 5% CO<sub>2</sub> before analysis.

### 5.5.3 Gymnosis

Cells were seeded at a density of  $5 \times 10^3$  per well in white TC-treated 96-well plates a day before treatment. Next day, media were replaced with fresh media containing 9 mM of CaCl<sub>2</sub>, together with or without an appropriate amount of oligonucleotide to achieve a 1 µM final concentration per well, following a previously reported protocol.<sup>107</sup> The medium was later (after 48–72 h) replaced with fresh medium containing 9 mM of CaCl<sub>2</sub>. Cells were incubated at 37 °C in a humidified incubator with 5% CO<sub>2</sub> and harvested for luciferase measurements 7 days after initial treatment.

### 5.5.4 Luciferase Assay

A modification of the previously reported protocol for the luciferase assay was followed.<sup>106</sup> The medium was removed, and the cells lysed in 25 µL of 0.1% Triton-X 100 in 1X PBS per well in a 96-well plate. After lysis of the cells, 5 µL aliquots of the lysates were used to determine total protein quantity by DC Protein Assay (BioRad). The remaining 20 µL of lysates were mixed with 50 µL of the luciferase reagent (Promega) added via injector. The relative light units (RLU) of luciferase were measured with a GloMax<sup>®</sup> 96 Microplate luminometer, with 10 s integration time and

2 s delay between injection and measurement. The observed values were divided by the total protein quantities determined and normalized to respective values of untreated wells. Final results are represented as fold increase in luciferase activity.

### 5.5.5 RNA Expression Analysis

For determination of expression levels of corrected luciferase mRNA, total RNA was isolated from the cells using the RNeasy plus kit. 3.0 ng of isolated RNA was used in each RT-PCR reaction using ONE STEP RT-PCR kit. The total volume was 20  $\mu$ L and the sequences of the forward and reverse primers were 5'-TTGATATGTGGATTTTCGAGTCGTC-3' and 5'-TGTC AATCAGAGTGCTTTTGGCG-3', respectively. The program for the RT-PCR was as follows: 35 min at 55 °C and 15 min at 95 °C for the reverse transcription, followed directly by 30 cycles of PCR (30 s at 94 °C, 30 s at 55 °C, and 30 s at 72 °C) and, finally, 10 min at 72 °C for the final extension. The PCR products were analyzed by gel electrophoresis in a 1.5% agarose gel and 1  $\times$  TBE buffer and visualized by SYBR Gold staining. Documentation of gels was done with the Versadoc imaging system equipped with a cooled CCD camera. Band intensities were analyzed with the Quantity One software and the percentage of corrected mRNA was calculated by normalization against the sum of band intensities of corrected and uncorrected bands.

### 5.5.6 Cell Viability Assay

The viability of cells after lipofection with the modified oligonucleotides was assessed with the WST-1 assay. Cells were seeded and transfected as described above. 24 h after transfection, the media were replaced with fresh media supplemented with the WST-1 reagent (1:10 dilution with H<sub>2</sub>O). After addition of media with the WST-1 reagent, the cells were further incubated for 2 h at 37 °C in a humidified incubator with 5% CO<sub>2</sub> according to the manufacturer's protocol. Absorbance measurements were carried out on a SpectraMAX i3x Western Blot Imager at  $\lambda = 450$  nm with a reference wavelength of 650 nm. Values were expressed as the ratio of the absorbance at 450 nm of the treated cells to the untreated cells.

### 5.5.7 Data Analysis

Data are expressed as mean  $\pm$  standard error of the mean (SEM). Statistical significance was determined by one- or two-way analysis of variance (ANOVA) followed by individual comparisons using Fisher's least significant difference test. In all cases,  $p < 0.05$  was considered significant.



# Acknowledgements

This thesis is based on experimental work performed in the Laboratory of Organic Chemistry and Chemical Biology at the Department of Chemistry, University of Turku, Finland as well as Department of Laboratory Medicine, Clinical Research Centre, Karolinska Institute, Huddinge, Sweden during the years of April 2017 to October 2021. The financial support from the European Union's Horizon 2020 research and innovation program under the Marie Skłodowska-Curie Grant, Department of Chemistry, University of Turku, Academy of Finland, Turku University Foundation, and Doctoral Programme in Physical and Chemical Sciences are gratefully acknowledged.

First and foremost, I am extremely grateful to my Ph.D. supervisor Associate Professor Tuomas Lönnberg for your nurturing supervision, constant support, and motivation. I have always benefited from your immense knowledge and experience in nucleic acid chemistry. You are not only THE best supervisor but also an incredible person to be around. I understand that supervision is as challenging as parenting and I must say you simply nailed it. I am sure I have did several stupid mistakes during these years and I never saw you reacting oddly. You were always very calm, patient, and nice to me. Because of this, I was always comfortable working with you. I have seen different shades of your personality and have no words to explain your level of patience. Seriously, how do you manage that? You stood by me in all uncertain times of my Ph.D. which is priceless. I am eternally grateful to have you as my Ph.D. guide. Thank you, thank you for everything.

I wish to thank Professor Zbigniew Leśnikowski and Professor Eva Freisinger for carefully evaluating my thesis. I am also thankful to Professor Anna Grandas for accepting to be my opponent. I reserve my special thanks to the Head of Chemistry Department and Bioorganic Group Professor Pasi Virta for your inspiration and helpful advice. I am very grateful for all the support that you have extended to me during my time in Finland.

I extend my gratitude to my collaborator Dr. Sajal Maity, Professor C. I. Edward Smith, Dr. Karin Lundin, Dr. Rula Zain, and Osama Saher for your invaluable support. I also want to thank Dr. Ulf Tedbark, and Kristina Druceikaite for all your cooperation during my short secondment in RISE, Sweden. I appreciate Dr. Liisa

van Vliet for coordinating the MMBio network training and meetings. They were truly helpful.

I have had the privilege to work with former and current members of the Bioorganic Group. I am very thankful to all for your cooperation and for maintaining a pleasant work culture: Dr. Dattatraya Ukale, Lange Yakubu Saleh, Dr. Ville Tähtinen, Petja Rosenqvist, Vijay Gulumkar, Asmo Aro-Heinilä, Aapo Aho, Antti Äärelä, Afari Mark, Dr. Emilia Kiuru, Dr. Heidi Korhonen, Dr. Lotta Granqvist, Dr. Mikko Ora, Dr. Satu Mikkola, Dr. Tharun Kumar Kotammagari and Tommi Österlund. I thank you all for being in my corner. Million thanks to Lange for being a friendly colleague and an amazing friend. Cheers to our endless brainy talks!

I am thankful to Kari Loikas, Kirsi Laaksonen and Mauri Nauma for always being there so that we can be fully functional. I must say that all our instruments bend to Mauri's will. You three are gems of the chemistry department. I also thank Dr. Jani Rakkila and Dr. Alex Dickens for your help in instrumentation.

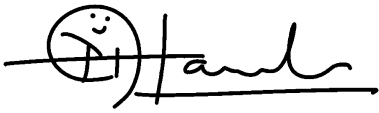
I am very thankful to my former supervisors Professor Saroj Ghaskadbi, Professor Suresh Gosavi, Associate Professor Anupa Kumbhar and Mr. Pradip Kharade for their support and motivation. I am grateful to my best teachers Dr. Abhijeet Papalkar, Dr. Sonalika Pawar and Dr. Rohitkumar Gore for encouraging me. I would have lost without your support. Your contribution to shape my career is huge. Thank you for all your guidance.

I am blessed with the wonderful people around me and I take this opportunity to acknowledge them. All of them have made a huge difference in my life. First of all, I want to thank you Ukale for always being a patient listener. You are such a soft-hearted person. Thank you for tolerating my all madness:D Despite many peaks and valleys, you are my partner in crime who has always stood by me for seven years now, and I hope we cross the paths again in the future. I wish you a very healthy life ahead. I acknowledge my energy boosters for keeping me sane and nostalgic all the time and they are the great Swapnil Dumbre, the great Varsha Teli, Sonal Ravale, Ashish Kamat, Nikhil Korhale and Sandhya Kumkar. Thank you for all those never-ending chats, talks and laughs. All these are crucial for my better mental health. Staying in a different country is equally adventurous as going on a roller coaster's ride. I am grateful to be with Foodie Fintians on this ride who made things easier to deal with: Amit Tewari, Dattatraya Ukale (again!), Ekansh Saxena, Neha Sharma, Prashali Bajpeyi, and Suvendu Rakshit, with me. Thank you Prashali, for all *VIP treatments* ♥ Guys, thank you for keeping my dopamine all-time high and kudos to our wonderful chemistry. You are a perfect blend of love affection and care. The time we spent in Finland is one of the most memorable times of my life. I love you so much and I will miss you a lot.

I am indebted to my parents Ashok and Nirmala, my sister Pooja, brother Vipul and my niece, our little champ Purva. Thank you Purva for your blind love to your

mau. You are our energy packet. Huge thanks to all of you because when I was doing a Ph.D., you all were doing a Ph.D. It was equally difficult for all of us to not see each other for the whole two years. Pappa, this ride started when I won the bet:P but thank you for always being on my side. Aai, you always have encouraged me to be a successful and independent woman, and I am trying... 😊 You both have always taken brave steps by giving me opportunities to explore my life in my way. I will not let you down ever for that. I miss you all ❤️

Last but not the least, I thank everyone who stood by me on this ride.

A handwritten signature in black ink. It starts with a circular doodle containing a simple face with two dots for eyes and a curved line for a smile. To the right of the doodle, the name 'Madhuri Ashok Hande' is written in a cursive, flowing script. The signature is underlined with a single horizontal line.

Madhuri Ashok Hande

Turku, October 2021

# List of References

- (1) Cech, T. R.; Zaug, A. J.; Grabowski, P. J. *Cell* **1981**.
- (2) Guerrier-Takada, C.; Gardiner, K.; Marsh, T.; Pace, N.; Altman, S. *Cell* **1983**.
- (3) Großhans, H.; Filipowicz, W. *Nature* **2008**.
- (4) Mattick, J. S. *PLoS Genetics*. 2009.
- (5) Watson, J. D.; Crick, F. H. *Nature* **2003**.
- (6) Brad Wan, W.; Seth, P. P. *J. Med. Chem.* **2016**, 59 (21), 9645–9667.
- (7) Alvey, H. S.; Gottardo, F. L.; Nikolova, E. N.; Al-Hashimi, H. M. *Nat. Commun.* **2014**, 5 (1).
- (8) Lippert, B. *Coordinative Bond Formation Between Metal Ions and Nucleic Acid Bases*; 2009.
- (9) Lippert, B.; Sanz Miguel, P. J. *Acc. Chem. Res.* **2016**, 49 (8), 1537–1545.
- (10) Shamsi, M. H.; Kraatz, H. B. *J. Inorg. Organomet. Polym. Mater.* **2013**, 23 (1), 4–23.
- (11) *Uses of Inorganic Chemistry in Medicine*; 2007.
- (12) Pyle, A. M.; Barton, J. K. 2007.
- (13) Jash, B.; Müller, J. *Chemistry - A European Journal*. 2017.
- (14) Kondo, J.; Tada, Y.; Dairaku, T.; Saneyoshi, H.; Okamoto, I.; Tanaka, Y.; Ono, A. *Angew. Chemie* **2015**, 127 (45).
- (15) Taherpour, S.; Lönnberg, H.; Lönnberg, T. *Org. Biomol. Chem.* **2013**, 11 (6), 991.
- (16) Schlegel, M. K.; Zhang, L.; Pagano, N.; Meggers, E. *Org. Biomol. Chem.* **2009**, 7 (3), 476–482.
- (17) Küsel, A.; Zhang, J.; Gil, M. A.; Stückl, A. C.; Meyer-Klaucke, W.; Meyer, F.; Diederichsen, U. *Eur. J. Inorg. Chem.* **2005**, No. 21.
- (18) Ma, Z.; Olechnowicz, F.; Skorik, Y. A.; Achim, C. *Inorg. Chem.* **2011**, 50 (13).
- (19) Katz, S. *Nature* **1962**.
- (20) KATZ, S. *Nature* **1962**, 194 (4828), 569–569.
- (21) Meggers, E.; Holland, P. L.; Tolman, W. B.; Romesberg, F. E.; Schultz, P. G. *Journal of the American Chemical Society*. 2000.
- (22) Kazakov, S. A.; Hecht, S. M. *Nucleic Acid-Metal Ion Interactions*; 2006.
- (23) Taherpour, S.; Golubev, O.; Lönnberg, T. *Inorganica Chim. Acta* **2016**, 452.
- (24) Taherpour, S.; Lönnberg, T. *J. Nucleic Acids* **2012**, 2012.
- (25) Tanaka, K.; Tengeiji, A.; Kato, T.; Toyama, N.; Shionoya, M. *Science (80-. )*. **2003**, 299 (5610).
- (26) Lippert, B. 2008.
- (27) Collado, A.; Gómez-Gallego, M.; Sierra, M. A. *European J. Org. Chem.* **2018**, 2018 (14), 1617–1623.
- (28) Stephenson, M. L.; Zamecnik, P. C. *Proc. Natl. Acad. Sci. U. S. A.* **1978**.
- (29) Marchán, V.; Grandas, A. *Met. Complex-DNA Interact.* **2009**, 273–300.
- (30) Edvard Smith, C. I.; Zain, R. *Annu. Rev. Pharmacol. Toxicol.* **2019**, 59, 605–630.
- (31) Xiong, H.; Veedu, R. N.; Diermeier, S. D. *International Journal of Molecular Sciences*. 2021.
- (32) Uhlmann, E.; Peyman, A. *Chem. Rev.* **1990**, 90 (4), 543–584.
- (33) Sanghvi, Y. S.; Cook, P. D. **1994**, 1–22.

- (34) Aboul-Fadl, T. *Curr. Med. Chem.* **2005**, *12* (19), 2193–2214.
- (35) Tanaka, M.; Nyce, J. W. *Respiratory Research*. 2001.
- (36) Deleavey, G. F.; Damha, M. J. *Chem. Biol.* **2012**, *19* (8), 937–954.
- (37) Roth, C. M.; Yarmush, M. L. *Annu. Rev. Biomed. Eng.* **1999**, No. 1, 265–297.
- (38) Ganju, A.; Khan, S.; Hafeez, B. B.; Behrman, S. W.; Yallapu, M. M.; Chauhan, S. C.; Jaggi, M. *Drug Discovery Today*. 2017.
- (39) Eichhorn, S. W.; Guo, H.; McGeary, S. E.; Rodriguez-Mias, R. A.; Shin, C.; Baek, D.; Hsu, S. hao; Ghoshal, K.; Villén, J.; Bartel, D. P. *Mol. Cell* **2014**.
- (40) Lennox, K. A.; Behlke, M. A. *Pharm. Res.* **2010**, *27* (9), 1788–1799.
- (41) Gebert, L. F. R.; Rebhan, M. A. E.; Crivelli, S. E. M.; Denzler, R.; Stoffel, M.; Hall, J. *Nucleic Acids Res.* **2014**.
- (42) Esquela-Kerscher, A.; Slack, F. J. *Nature Reviews Cancer*. 2006.
- (43) Shah, M. Y.; Ferrajoli, A.; Sood, A. K.; Lopez-Berestein, G.; Calin, G. A. *EBioMedicine* **2016**, *12*, 34–42.
- (44) Allan Drummond, D.; Wilke, C. O. *Nature Reviews Genetics*. 2009.
- (45) Thakur, P. K.; Rawal, H. C.; Obuca, M.; Kaushik, S. In *Encyclopedia of Bioinformatics and Computational Biology*; Elsevier, 2019; pp 221–234.
- (46) Mezhevaya, K.; Winters, T. A.; Neumann, R. D. *Nucleic Acids Res.* **1999**.
- (47) Gissberg, O. I.; Jezowska, M.; Zaghoul, E. M.; Bungsu, N. I.; Strömberg, R.; Smith, C. I. E.; Lundin, K. E.; Honcharenko, M. *Org. Biomol. Chem.* **2016**.
- (48) Song, K. M.; Lee, S.; Ban, C. *Sensors*. 2012.
- (49) Schnee, M.; Vogel, A. B.; Voss, D.; Petsch, B.; Baumhof, P.; Kramps, T.; Stitz, L. *PLoS Negl. Trop. Dis.* **2016**, *10* (6).
- (50) Chahal, J. S.; Fang, T.; Woodham, A. W.; Khan, O. F.; Ling, J.; Anderson, D. G.; Ploegh, H. L. *Sci. Rep.* **2017**, *7* (1).
- (51) Van Craenenbroeck, A. H.; Smits, E. L. J.; Anguille, S.; Van de Velde, A.; Stein, B.; Braeckman, T.; Van Camp, K.; Nijs, G.; Ieven, M.; Goossens, H.; Berneman, Z. N.; Van Tendeloo, V. F. I.; Verpooten, G. A.; Van Damme, P.; Cools, N. *Transplantation* **2015**, *99* (1).
- (52) Pardi, N.; Hogan, M. J.; Porter, F. W.; Weissman, D. *Nat. Rev. Drug Discov.* **2018**, *17* (4).
- (53) Wolff, J.; Malone, R.; Williams, P.; Chong, W.; Acsadi, G.; Jani, A.; Felgner, P. *Science (80- )*. **1990**, *247* (4949).
- (54) Roberts, T. C.; Langer, R.; Wood, M. J. A. *Nat. Rev. Drug Discov.* **2020**, *19* (10).
- (55) Kool, E. T. *Acc. Chem. Res.* **2002**, *35* (11), 936–943.
- (56) Kawasaki, A. M.; Casper, M. D.; Freier, S. M.; Lesnik, E. A.; Zounes, M. C.; Cummins, L. L.; Gonzalez, C.; Dan Cook, P. *J. Med. Chem.* **1993**.
- (57) Obika, S.; Nanbu, D.; Hari, Y.; Andoh, J. I.; Morio, K. I.; Doi, T.; Imanishi, T. *Tetrahedron Lett.* **1998**.
- (58) Leumann, C. J. *Bioorganic and Medicinal Chemistry*. 2002.
- (59) Khvorova, A.; Watts, J. K. *Nat. Biotechnol.* **2017**, *35* (3), 238–248.
- (60) De Mesmaeker, A.; Waldner, A.; Lebreton, J.; Hoffmann, P.; Fritsch, V.; Wolf, R. M.; Freier, S. M. *Angew. Chemie Int. Ed. English* **1994**, *33* (2), 226–229.
- (61) DeVos, S. L.; Miller, T. M. *Neurotherapeutics* **2013**, *10* (3), 486–497.
- (62) Micklefield, J. *Curr. Med. Chem.* **2012**, *8* (10), 1157–1179.
- (63) De Mesmaeker, A.; Waldner, A.; Lebreton, J.; Fritsch, V.; Wolf, R. M. **1994**, 24–39.
- (64) Summerton, J. *Curr. Top. Med. Chem.* **2007**, *7* (7), 651–660.
- (65) Gryaznov, S.; Skorski, T.; Cucco, C.; Nieborowska-Skorska, M.; Chiu, C. Y.; Lloyd, D.; Chen, J. K.; Koziolkiewicz, M.; Calabretta, B. *Nucleic Acids Res.* **1996**, *24* (8), 1508–1514.

- (66) Heasman, J. *Developmental Biology*. 2002.
- (67) Seela, F.; He, Y.; He, J.; Becher, G.; Kröschel, R.; Zulauf, M.; Leonard, P. *Methods Mol. Biol.* **2005**.
- (68) Stambaský, J.; Hocek, M.; Kočovský, P. *Chem. Rev.* **2009**, *109* (12), 6729–6764.
- (69) Shaughnessy, K. H. *Molecules*. 2015.
- (70) Omumi, A.; Beach, D. G.; Baker, M.; Gabryelski, W.; Manderville, R. A. *J. Am. Chem. Soc.* **2011**.
- (71) Peyrone, M. *Ann. der Chemie und Pharm.* **1844**, *51* (1).
- (72) Werner, A. *Zeitschrift für Anorg. Chemie* **1893**, *3* (1).
- (73) ROSENBERG, B.; VAN CAMP, L.; KRIGAS, T. *Nature* **1965**, *205* (4972).
- (74) Wilson, J. J.; Lippard, S. J. *Chem. Rev.* **2014**, *114* (8), 4470–4495.
- (75) Alguero, B.; López De La Osa, J.; González, C.; Pedroso, E.; Marchán, V.; Grandas, A. *Angew. Chemie - Int. Ed.* **2006**, *45* (48).
- (76) Giraud-Panis, M. J.; Leng, M. In *Pharmacology and Therapeutics*; 2000; Vol. 85.
- (77) Boudvillain, M.; Guérin, M.; Dalbiès, R.; Saison-Behmoaras, T.; Leng, M. *Biochemistry* **1997**, *36* (10).
- (78) Gee, J. E.; Robbins, I.; Van Der Laan, A. C.; Van Boom, J. H.; Colombier, C.; Leng, M.; Raible, A. M.; Nelson, J. S.; Lebleu, B. *Antisense Nucleic Acid Drug Dev.* **1998**, *8* (2).
- (79) Colombier, C.; Lippert, B.; Leng, M. *Nucleic Acids Res.* **1996**, *24* (22).
- (80) Schmidt, K. S.; Boudvillain, M.; Schwartz, A.; Van der Marel, G. A.; Van Boom, J. H.; Reedijk, J.; Lippert, B. *Chem. - A Eur. J.* **2002**, *8* (24).
- (81) Dale, R. M. K.; Livingston, D. C.; Ward, D. C. *Proc. Natl. Acad. Sci. U. S. A.* **1973**, *70* (8).
- (82) Kowalski, K. *Coordination Chemistry Reviews*. 2021.
- (83) Martín-Ortiz, M.; Gómez-Gallego, M.; Ramírez De Arellano, C.; Sierra, M. A. *Chem. - A Eur. J.* **2012**, *18* (40).
- (84) Ito, Y.; Mizuno, K.; Domoto, K.; Hari, Y. *Nucleosides, Nucleotides and Nucleic Acids* **2020**, *39* (1–3).
- (85) Shao, F.; Barton, J. K. *J. Am. Chem. Soc.* **2007**, *129* (47).
- (86) Valencia, M.; Merinero, A. D.; Lorenzo-Aparicio, C.; Gómez-Gallego, M.; Sierra, M. A.; Eguillor, B.; Esteruelas, M. A.; Oliván, M.; Onáte, E. *Organometallics* **2020**, *39* (2).
- (87) Cerón-Camacho, R.; Roque-Ramires, M. A.; Ryabov, A. D.; Le Lagadec, R. *Molecules*. 2021.
- (88) Scattolin, T.; Voloshkin, V. A.; Visentin, F.; Nolan, S. P. *Cell Reports Physical Science*. 2021.
- (89) Tanaka, K.; Shionoya, M. *J. Org. Chem.* **1999**, *64* (14).
- (90) Maity, S.; Hande, M.; Lönnberg, T. *ChemBioChem* **2020**, *21* (16), 2321–2328.
- (91) Maity, S. K.; Lönnberg, T. A. *ACS Omega* **2019**.
- (92) Hande, M.; Saher, O.; Lundin, K. E.; Edvard Smith, C. I.; Zain, R.; Lönnberg, T. *Molecules* **2019**, *24* (6).
- (93) Hande, M.; Maity, S.; Lönnberg, T. *Int. J. Mol. Sci.* **2018**, *19* (6).
- (94) Maity, S. K.; Lönnberg, T. *Chem. - A Eur. J.* **2018**, *24* (6), 1274–1277.
- (95) Hande, M.; Maity, S.; Lönnberg, T. *Int. J. Mol. Sci.* **2018**, *19* (6).
- (96) Hande, M.; Saher, O.; Lundin, K. E.; Edvard Smith, C. I.; Zain, R.; Lönnberg, T. *Molecules* **2019**.
- (97) Hande, M.; Maity, S.; Lönnberg, T. *J. Inorg. Biochem.* **2021**, *222*.
- (98) Golubev, O.; Turc, G.; Lönnberg, T. *J. Inorg. Biochem.* **2016**, *155*, 36–43.
- (99) Maity, S. K.; Lönnberg, T. *Chem. - A Eur. J.* **2018**.
- (100) Mergny, J. L.; Lacroix, L. *Oligonucleotides*. 2003.
- (101) Ukale, D.; Shinde, V. S.; Lönnberg, T. *Chem. - A Eur. J.* **2016**, *22* (23).

- (102) Torigoe, H.; Ono, A.; Kozasa, T. *Chem. - A Eur. J.* **2010**, *16* (44).
- (103) Aro-Heinilä, A.; Lönnberg, T.; Virta, P. *Bioconjug. Chem.* **2019**, *30* (8).
- (104) Dominski, Z.; Kole, R. *Proc. Natl. Acad. Sci. U. S. A.* **1993**, *90* (18).
- (105) Kang, S. H.; Cho, M. J.; Kole, R. *Biochemistry* **1998**, *37* (18).
- (106) Rocha, C. S. J.; Lundin, K. E.; Behlke, M. A.; Zain, R.; EL Andaloussi, S.; Smith, C. I. E. *Nucleic Acid Ther.* **2016**, *26* (6), 381–391.
- (107) Hori, S. I.; Yamamoto, T.; Waki, R.; Wada, S.; Wada, F.; Noda, M.; Obika, S. *Nucleic Acids Res.* **2015**, *43* (19).



**TURUN  
YLIOPISTO**  
UNIVERSITY  
OF TURKU

ISBN 978-951-29-8672-9 (PRINT)  
ISBN 978-951-29-8673-6 (PDF)  
ISSN 0082-7002 (Print)  
ISSN 2343-3175 (Online)